공학박사 학위논문

Low-Complexity Blind SLM and PTS Schemes for PAPR Reduction of OFDM Systems

OFDM 시스템의 PAPR 감소를 위한 저연산량을 갖는 블라인드 SLM 및 PTS 기법에 관한 연구

2012년 8월

서울대학교 대학원

전기컴퓨터공학부

주 현 승

Abstract

Low-Complexity Blind SLM and PTS Schemes for PAPR Reduction of OFDM Systems

Hyun-Seung Joo
Department of EE and CS
The Graduate School
Seoul National University

In this dissertation, several research results for the peak-to-average power ratio (PAPR) reduction schemes with low complexity for the orthogonal frequency division multiplexing (OFDM) signals are discussed. First, the basic principle, performance, and implementation of the OFDM systems are introduced. OFDM signal with the high PAPR is described, which is one of main drawbacks of OFDM. Many PAPR reduction schemes to solve this problem have been studied such as clipping, coding, selected mapping (SLM), partial transmit sequence (PTS), tone reservation, and tone injection.

In the first part of this dissertation, blind SLM (BSLM) scheme is proposed for OFDM systems. The proposed BSLM scheme embeds the side information (SI) identifying a phase sequence into itself by giving the phase offset to the elements of each phase sequence, which are deter-

mined by any set of vectors for the partitioned subblocks. When U phase sequences and maximum likelihood (ML) decoder are used, the proposed BSLM scheme reduces the decoding complexity by $(U-2)/U$ compared to the conventional BSLM scheme. The detection failure probability (DFP) of the SI for the proposed BSLM scheme is derived and the closed-form expression of DFP is obtained for $U = 4$ and 8 over additive white Gaussian noise channel. Also, pairwise error probability (PEP) analysis for the proposed BSLM scheme is derived over the fading channel. Based on the PEP analysis, we show that bit error rate (BER) performance of the proposed BSLM scheme is determined by phase offset vectors and phase offset. Finally, it is shown that for QPSK and 16-QAM, the DFP and the bit error rate of the proposed BSLM scheme are almost the same as those of the conventional BSLM scheme through numerical analysis.

In addition, we propose two blind PTS (BPTS) schemes for PAPR reduction of OFDM signals. Similar to the proposed BSLM scheme, the proposed BPTS schemes embeds the SI identifying a rotating vector into itself by using the phase offset on the elements of each rotating vector. To extract SI from the rotating vector and recover the data sequence, the ML decoders for the proposed BPTS schemes without SI are derived. These decoders exploit the fact that the Euclidean distance between the given signal constellation and the signal constellation rotated by the phase offset exists. By using PEP analysis, it is explained how phase offsets for each BPTS scheme should be chosen. Finally, it is shown that for QPSK and 16-QAM, the BER performance of the proposed BPTS schemes without

SI is not degraded through the simulation results.

In the second part of this dissertation, a new subblock partitioning scheme with low complexity using the subblock partition matrix for OFDM systems is proposed, which can be applied to the PAPR reduction scheme for PTS, the interleaved orthogonal frequency division multiple access (OFDMA) systems, and the multi-input multi-output (MIMO) OFDM system with space frequency block coding (SFBC). Based on the convolution property of the inverse fast Fourier transform (IFFT), the subblock partition matrix can be derived. The IFFTed signal subsequences are generated from the circular convolution of the OFDM signal sequence in the time domain and the column vector of the subblock partition matrix. Since several IFFT operations of the signal subsequences are replaced by the convolution of the OFDM signal sequence in the time domain with the column vector of the proposed subblock partition matrix, only one IFFT operation is required, which means that their computational complexity is reduced. The interleaved subblock partitioning scheme is suitable for the proposed subblock partition matrix in terms of complexity reduction.

Keywords: Blind selected mapping (BSLM), blind partial transmit sequence (BPTS), orthogonal frequency division multiplexing (OFDM), peak-to-average power ratio (PAPR), side information (SI), subblock partitioning.

Student ID: 2008-30888

Contents

List of Tables

List of Figures

Chapter 1. Introduction

1.1. Background

Recently, wireless communication systems have been developed through research of communication theory and technology. Since the demand for multimedia service is growing exponentially, the communication systems have to support high data rate and high reliability to provide such services. Orthogonal frequency division multiplexing (OFDM) is a multi-carrier modulation technique which offers good performance and several benefits because it can achieve high data transmission and insure high reliability over the multipath fading environment. Due to these advantages, OFDM has been adopted as the standards for various wireless communication systems being used and developed today such as IEEE 802.11a/g (WLANs), digital audio broadcasting (DAB), digital video broadcasting (DVB), IEEE 802.16 (WiMAX), and LTE.

OFDM is based on the frequency-division multiplexing (FDM), the method to transmit multiple data streams over a common spectrum. Each data stream is modulated onto multiple carriers within the bandwidth of the spectrum. In other words, the serial data stream for transmission is split into multiple low data streams, and each is modulated onto a separate carrier in the orthogonal manner within the assigned spectrum. These

carriers are called subcarriers or tones. All the subcarriers are linearly summed and the OFDM signal is generated for transmission.

The concept of OFDM has been introduced around the 1950s, which was known as a multicarrier modulation, as opposed to the traditional single-carrier modulation. In 1968, Chang and Gibby suggested a parallel transmission scheme using orthogonal multiplexing [1]. However, OFDM was extremely difficult to implement with the electronic hardware at the time. Thus, it remained an incomplete research area until semiconductor and computer technology were developed. In 1971, Weinstein devised the parallel data transmission system by using inverse discrete Fourier transform (IDFT), and then, it can be effectively implemented by inverse fast Fourier transform (IFFT) [2]. In 1980, it was proposed that OFDM symbol can be cyclically extended in the guard time [3]. It can remove both inter-symbol interference (ISI) and inter-carrier interference (ICI).

The parallel transmission of OFDM increases the symbol duration and it makes frequency selective fading channel to several flat fading channels. Therefore, OFDM has the immunity from frequency selective fading channel. In the OFDM system with guard interval, the complex equalizer is not required because the one-tap equalizer compensates the signal distortion over the fading channel. Also, OFDM has an advantage of the spectral efficiency due to subcarrier orthogonality. OFDM subchannels whose spectra satisfy orthogonality can be overlapped each other, which saves the spectral efficiency up to 50%. The spectral overlapping for the OFDM signal is possible because subcarriers are orthogonal. With excellent spec-

tral efficiency, OFDM has become worthy in the wireless communication area.

Due to the advantages, OFDM is an popular technique in the wireless communication systems with high data rate over the frequency selective fading channel environments. However, it has several drawbacks such as high sensitivity to inter-channel interference, I/Q mismatch, and high peak-to-average power ratio (PAPR) of OFDM signals. Specially, a high PAPR of OFDM signals leads to significant inter-modulation and out-of-band radiation when OFDM signals passes through nonlinear devices such as high power amplifier (HPA) [4]. Since linear range of HPA is limited, peak power of OFDM signals in time domain should be reduced.

Several techniques have been proposed to mitigate the PAPR of OFDM signals. Clipping the signal peaks is the simplest PAPR reduction method and is used in most of today's OFDM system implementations [5]. Even though clipping is very popular method, it causes in-band distortion and out-of-band radiation. Tone reservation (TR) [6] and tone injection (TI) [6] modify OFDM signals, which peak canceling signals are added. Peak canceling signals change signal constellation points in a part of subcarriers for PAPR reduction. The drawbacks of them are to degrade data rate or to increase transmission power. And symbol scrambling techniques such as selected mapping (SLM) and partial transmit sequences (PTS) for PAPR reduction exist with no signal distortions [7]–[12]. The key idea of SLM and PTS is that for each OFDM symbol, the OFDM signal sequence with the minimum PAPR is selected for transmission from the U alternative

signal sequences which are scrambled by U phase sequences. When the number of alternative signal sequences in the SLM and PTS increases, the possibility to improve the PAPR reduction performance is more insured. However, the computational complexity also increases from several IFFT operations. Also, in the SLM and PTS, the side information (SI) must be transmitted to allow the recovery of original symbol sequence at the receiver, which reduces the data transmission rate. An erroneous detection of the SI causes a significant degradation on the bit error rate (BER). Therefore, strong protection for the SI is required and causes more loss of data transmission rate occurs. To remove the transmission of such SI, several blind schemes for SLM and PTS have been proposed [13]–[16]. These proposed techniques insert some additional reference symbols to pilot symbols or have large decoding complexity to recover the input symbol sequence.

1.2. Overview of Dissertation

The rest of this dissertation is organized as follows. In Chapter 2, OFDM system model is defined and the characteristic of HPA is introduced. And thus, PAPR is defined for baseband and passband OFDM signals, respectively. In Chapter 3, several PAPR reduction schemes for OFDM systems and their low-complexity algorithms are briefly explained.

In Chapter 4, a new blind SLM (BSLM) scheme with low decoding complexity is proposed. In the proposed BSLM scheme, the SI is embedded into each phase sequence by giving the phase offset to the elements

of the phase sequence, which is determined by the biorthogonal vectors for the partitioned subblocks. An maximum likelihood (ML) decoder with low decoding complexity is derived for the proposed BSLM scheme, which reduces the decoding complexity by $(U-2)/U$ compared with the conventional BSLM scheme in [15]. The detection failure probability (DFP) of the SI for the proposed BSLM scheme is derived and the closed-form expression of DFP is obtained for $U = 4$ and 8 over additive white Gaussian noise (AWGN) channel. Also, pairwise error probability (PEP) analysis for the proposed BSLM scheme is derived over the fading channel. Based on the PEP analysis, BER performance of the proposed BSLM scheme is shown to be determined by subblock partitioning and phase offset. Also, the numerical results show that for the OFDM systems with QPSK and 16-QAM, the DFP and BER of the proposed BSLM scheme are almost the same as those of the conventional BSLM scheme.

In Chapter 5, two blind PTS (BPTS) schemes are also proposed. In the proposed BPTS schemes, the SI is embedded into each rotating vector by giving the phase offset to the elements of the rotating vector similar to the proposed BSLM in Chapter 4. New ML decoders for the proposed BPTS schemes to recover original data from phase offsets are also proposed. PEP analysis for the proposed BPTS scheme is derived over the fading channel. Based on the PEP analysis, the number of phase offset is derived in order to improve BER performance of the proposed BPTS scheme. Simulation results show that for the OFDM systems with QPSK and 16-QAM, the ML decoders in the proposed BPTS schemes are well behaved.

In Chapter 6, we propose a new subblock partitioning scheme with low complexity using the subblock partition matrix in OFDM systems, which can be used for orthogonal frequency-division multiple access (OFDMA) system and PTS scheme. Using the convolution property of the IFFT, the subblock partition matrix is derived. The signal subsequences are obtained by the circular convolution of the OFDM signal sequence and the column vector of the subblock partition matrix in the time domain. IFFT operations to generate V signal subsequences are replaced by the circular convolution of the OFDM signal sequences in the time domain and the column vector of the subblock partition matrix, and thus, only one IFFT operation is required without additional IFFT operations. It is shown that the interleaved subblock partitioning scheme is suitable for the use of the subblock partition matrix because the elements of the subblock partition matrix are almost zero.

Finally, some concluding remarks are given in Chapter 7. The proposed techniques in the dissertation are reviewed and their further works are discussed.

Chapter 2. OFDM Systems

In order for data rates to achieve capacity over diverse channels, wireless communication systems have to adopt several transmission schemes such as coding, pulse shaping with modulation, and equalization. However, the high rate data transmission system is not easy to be implemented using a single-carrier system. As an alternative scheme, a multicarrier modulation, called OFDM, has been proposed.

The main idea of OFDM is to split the high data rate stream into N substream with low data rate and to transmit these substream data on N adjacent subcarriers. Since the data symbols are allocated in parallel over the frequency domain, the total bandwidth to transmit these symbols is not changed. Therefore, a symbol duration increases by a factor of N and thus, transmission with N times higher data rate for a given delay spread is possible. Moreover, from the parallel transmission over the frequency selective fading channel, the OFDM system can alleviate the ISI of the single-carrier system in the multipath fading channel. As spreading out a frequency selective fading over N symbols, it leads to scattering effectively burst errors caused by fading or impulse noise so that instead of a few adjacent symbols being completely destroyed, N symbols are only slightly distorted.

Although OFDM is robust to the frequency selective fading and provides spectral efficiency, a main drawback of OFDM is the high PAPR. High PAPR implies that HPA must have an inefficiently large linear range. An amplifier with a wide linear operation region is very expensive and its cost occupies more than 20% of total cost of transmitter. Therefore, PAPR of OFDM signals should be reduced to avoid the BER degradation and out-of-band radiation in the HPA.

In this chapter, the mathematical representation of OFDM system is described. Also, the input-output characteristic of HPA is introduced. This chapter is organized as follows. In Section 2.1, we describe the mathematical representation of OFDM system. In Section 2.2, the high power amplifier model is introduced. Finally, PAPR is defined in the OFDM system and its relations are explained in Section 2.3.

2.1. System Model

OFDM converts a high rate data stream into many low rate data streams by dividing wideband spectrum. That is, the high rate data stream is split into N low rate data streams, modulated using N subcarriers, and transmitted over the channel. Each low rate data stream is loaded on the subcarrier and all the N subcarriers are summed for transmission. Generally, the input binary data is encoded by a channel code such as turbo code and convolutional code. The encoded bitstream is mapped into an input symbol sequence $\mathbf{X} = [X_0 \ X_1 \ \cdots \ X_{N-1}]^T$ modulated by M-ary phase shift keying (M-PSK) or M-ary quadrature amplitude modulation

(M-QAM), where N is the number of subcarriers and $(\cdot)^T$ denotes the transpose of a vector. And then, the baseband continuous time OFDM signal can be expressed as

$$x(t) = \frac{1}{\sqrt{N}} \sum_{k=0}^{N-1} X_k e^{j2\pi\Delta f k t}, \quad 0 \le t \le T_u \tag{2.1}$$

where Δf is the frequency spacing between adjacent subcarriers and T_u is the OFDM symbol duration without guard interval. The relation between Δf and T_u has $\Delta f = 1/T_u$.

In OFDM systems, loading the symbols on the subcarriers is practically implemented by IFFT. All subcarriers can be easily separated because subcarriers are orthogonal each other. An oversampled OFDM symbol sequence in the frequency domain is expressed as $\mathbf{X} = [X_0 \ X_1 \ \cdots \ X_{N-1} \ \underbrace{0 \cdots 0}_{(L-1)N}]^T$ by padding $(L-1)N$ zeros at the end of the input symbol sequence, where L is oversampling factor. Let $\mathbf{x} = [x_0 \ x_1 \ \cdots \ x_{LN-1}]^T$ denotes the oversampled baseband discrete time OFDM signal sequence. Therefore, the baseband discrete time OFDM signal can be expressed as

$$x_n = \frac{1}{\sqrt{N}} \sum_{k=0}^{N-1} X_k e^{j\frac{2\pi nk}{LN}}, \quad 0 \le n < LN. \tag{2.2}$$

When $L = 1$, the OFDM signal is sampled by Nyquist rate. It is known that the oversampled OFDM signal is considered to investigate the PAPR of discrete time OFDM signals because the Nyquist rate sampled OFDM signals do not exactly represent PAPR of the continuous time OFDM signals.

After OFDM signals pass through the channel, the received passband OFDM signal at the receiver is first down-converted to a baseband continuous time OFDM signal. And then, it can be sampled to the baseband discrete time OFDM signal r_n by a analog-to-digital converter (ADC). Therefore, the received OFDM symbol $\hat{X}_k$ is obtained by fast Fourier transform (FFT) as

$$\hat{X}_k = \frac{1}{\sqrt{N}} \sum_{n=0}^{LN-1} r_n e^{-j\frac{2\pi nk}{LN}}, \quad 0 \le k < N. \tag{2.3}$$

After the received OFDM signals pass through frequency domain equalizer, demodulator, and channel decoder, the output binary information is finally obtained at the receiver.

IFFT expression of (2.2) can be written in an $LN \times LN$ IFFT matrix as

$$\mathbf{Q} = \frac{1}{\sqrt{N}} \begin{bmatrix} 1 & 1 & 1 & \cdots & 1 \\ 1 & W_{LN}^{-1} & W_{LN}^{-2} & \cdots & W_{LN}^{-(N-1)} \\ 1 & W_{LN}^{-2} & W_{LN}^{-4} & \cdots & W_{LN}^{-2(N-1)} \\ \vdots & \vdots & \vdots & \ddots & \vdots \\ 1 & W_{LN}^{-(N-1)} & W_{LN}^{-2(N-1)} & \cdots & W_{LN}^{-(N-1)\times(N-1)} \end{bmatrix} \tag{2.4}$$

with $W_{LN} = e^{-j\frac{2\pi}{LN}}$. Also, FFT expression of (2.2) can be expressed as $\mathbf{Q}^{-1}$. Therefore, the vector expressions of OFDM signal sequence and

OFDM symbol sequence are given as

$$\mathbf{x} = \mathbf{Q}\mathbf{X} \tag{2.5}$$

and

$$\mathbf{X} = \mathbf{Q}^{-1}\mathbf{x}, \tag{2.6}$$

respectively.

2.2. High Power Amplifier Models

A simplified input-output relationship of the nonlinear HPA for a base-band OFDM signal is expressed as

$$s_{out}(t) = G[|x(t)|]e^{j(\phi_x(t)+\Phi[|x(t)|])} \tag{2.7}$$

where the functions $G[\cdot]$ and $\Phi[\cdot]$ denote the AM/AM and AM/PM distortion, respectively. Typical models for characterizing HPA are introduced as follows.

2.2.1. TWTA

The AM/AM and AM/PM conversion functions of the traveling wave tube amplifier (TWTA) model are obtained by using an approximation with the two-parameter formulas

$$G[|x(t)|] = \frac{\alpha_G|x(t)|}{1+\beta_G|x(t)|^2} \tag{2.8}$$

and

$$\Phi[|x(t)|] = \frac{\alpha_\Phi |x(t)|^2}{1 + \beta_\Phi |x(t)|^2} \tag{2.9}$$

where α_G, β_G, α_Φ, and β_Φ determine the characteristics of TWTA [17].

2.2.2. SSPA

The typical solid state power amplifier (SSPA) has more linear behavior in the small region than TWTA [18]. For large inputs, the AM/AM conversion function $G[|x(t)|]$ approaches to the maximum limiting value produced by current and voltage clipping. The AM/PM conversion of SSPA is assumed to be small enough so that it can be neglected. The AM/AM conversion function $G[|x(t)|]$ is expressed as

$$G[|x(t)|] = \frac{g_0 |x(t)|}{[1 + (|x(t)|/a_{sat})^2 p]^{1/2p}} \tag{2.10}$$

and

$$\Phi[|x(t)|] = 0 \tag{2.11}$$

where g_0 is the small signal gain, a_{sat} is the input saturation level, and p determines the smoothness of the transition from the linear region to the saturation region.

2.3. Peak-to-Average Power Ratio

Since OFDM signals are generated by summing N subcarriers, the peak power of OFDM signals can be very large compared to its average power

when N subcarriers are added up coherently. When it passes through non-linear device such as HPA, high peak power leads to distortion of OFDM signal, which causes in-band distortion and out-of-band radiation. The in-band distortion degrades BER and the out-of-band radiation interferes with the signals in the adjacent frequency bands. Therefore, it is very important to reduce peak power of OFDM signals.

2.3.1. Definition of PAPR

The PAPR of the oversampled discrete time OFDM signal is defined as the ratio of the maximum peak power to the average power of the OFDM signal [8], that is,

$$\mathrm{PAPR}(x_n) \triangleq \frac{\max\limits_{0 \le n \le LN-1} |x_n|^2}{P_{\mathrm{av}}(x_n)} \tag{2.12}$$

where $\mathrm{E}[\cdot]$ denotes the expectation and $P_{\mathrm{av}}(x_n) = \mathrm{E}[|x_n|^2]$. We assume that the input symbols are identically and independently distributed and the average power $P_{\mathrm{av}}(x_n)$ of input symbols is σ^2.

The PAPR of the continuous time OFDM signal $x(t)$ defined as the ratio of the maximum instantaneous power divided by the average power of the OFDM signal can be expressed as

$$\mathrm{PAPR}(x(t)) \triangleq \frac{\max\limits_{0 \le t < T_u} |x(t)|^2}{P_{\mathrm{av}}(x(t))}$$

where $P_{\mathrm{av}}(x(t)) = \mathrm{E}[|x(t)|^2]$.

Finally, another measure of the envelope variation of the OFDM signals

is the crest factor ζ, which is the ratio of the maximum to the root mean square of the signal envelope defined by

$$\zeta(x_n) \triangleq \frac{\max\limits_{0 \le n \le LN-1} |x_n|}{\sqrt{P_{\text{av}}(x_n)}}.$$

The discrete time OFDM signals as the output of the IFFT block are up-converted to the continuous time OFDM signals by the digital to analog converter (DAC), where the peak powers can be increased. It is known that the PAPR of the continuous time OFDM signals is larger than that of the discrete time OFDM signals by about 1.0 dB. Therefore, the discrete time OFDM signals should be oversampled to approximate the continuous time OFDM signals. It is shown that PAPR of the oversampled discrete time OFDM signals can approximate that of the continuous time OFDM signals when the oversampling factor L is more than 4 because the error due to the sampling is bounded by [19]

$$|\max_{0 \le t < T_u} |x(t)| - \max_{0 \le n < LN} |x_n|| \le N[\cos^{-1}(\pi/2L) - 1]. \tag{2.13}$$

2.3.2. Distribution of PAPR

For large N, the real and imaginary parts of x_n have complex Gaussian random distribution by central limit theorem. Since $r_n = |x_n|$ becomes a Rayleigh distributed random variable, the probability that the magnitude

of all N OFDM samples are smaller than certain threshold γ_0 is given as

$$\Pr\left(\max_{0\leq n\leq N-1} r_n < \gamma_0\right) = \Pr(r_n < \gamma_0)^N = (1 - e^{-\gamma_0^2})^N. \tag{2.14}$$

From (2.14), the probability that at least one magnitude of the OFDM signal samples exceeds a certain magnitude threshold γ_0 can be approximated as

$$\Pr(\text{PAPR} > \gamma_0) = 1 - (1 - e^{-\gamma_0^2})^N. \tag{2.15}$$

However, from the Gaussian approximation, the distribution in (2.15) does not match exactly with the numerical results in the continuous time OFDM signals. In [20], the empirical approximation was suggested as

$$\Pr(\text{PAPR} > \gamma_0) = 1 - (1 - e^{-\gamma_0^2})^{\alpha N} \tag{2.16}$$

where Nee proposed that (2.16) is the most agreeable with continuous time result when $\alpha = 2.8$. Also, Ochiai derived the PAPR distribution of the continuous time OFDM signal $x(t)$ as [21]

$$\Pr(\text{PAPR} > \gamma_0) \approx 1 - \exp\left(-\sqrt{\frac{\pi}{3}} N \gamma_0 e^{-\gamma_0^2}\right). \tag{2.17}$$

Fig. 2.1 shows the simulation results and (2.15) for the complementary cumulative distribution function (CCDF) of PAPR distribution for OFDM signal with $L = 1$ and $M = 16$ for various N. It is easy to check that PAPR becomes larger as N increases. Fig. 2.2 shows the CCDF of PAPR

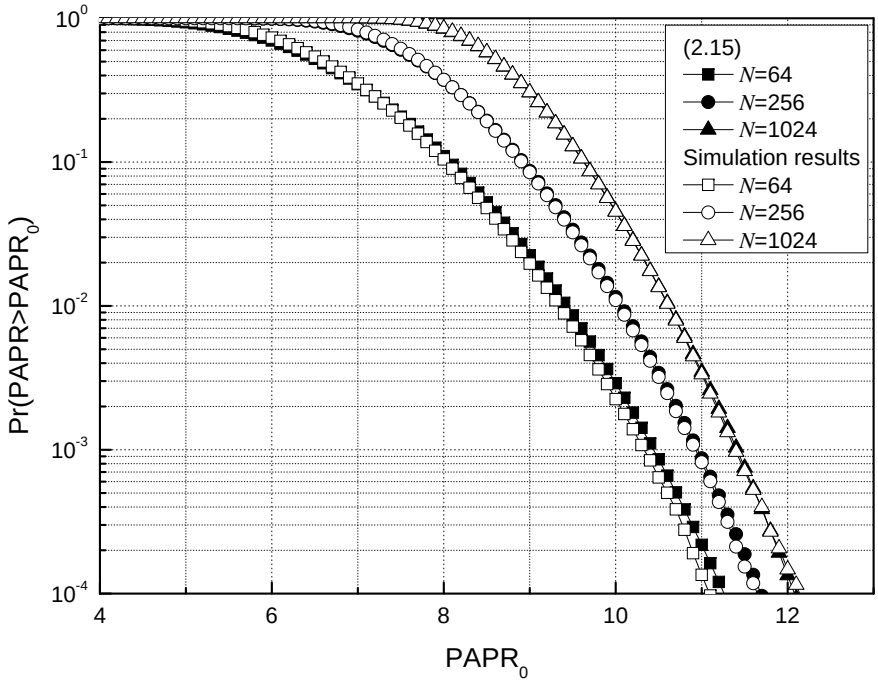

Figure 2.1: CCDF of PAPR distribution of OFDM signals with $N = 64$, 256, and 1024.

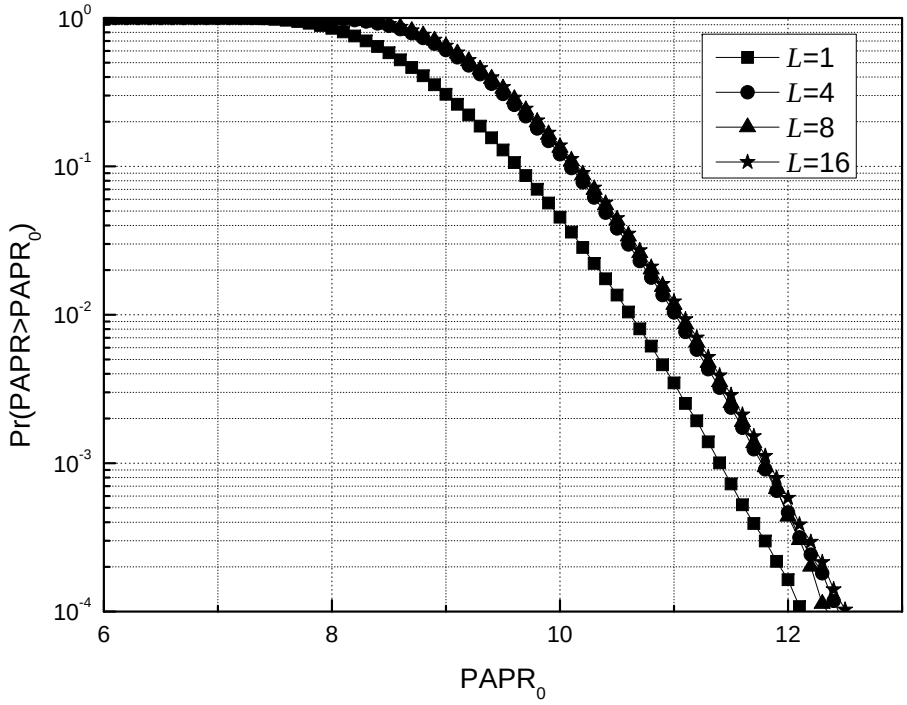

Figure 2.2: CCDF of PAPR distribution of OFDM signals with $L = 1$, 4, 8, and 16.

distribution for OFDM signal with $N = 1024$ and $M = 16$ for various oversampling factors L. It is shown that PAPR distribution of OFDM signal with 4 times oversampling rate is almost the same as that of the continuous time OFDM signals.

Chapter 3. PAPR Reduction Schemes

It has been known that the PAPR problem is an important issue in OFDM systems. Thus, several PAPR reduction schemes have been proposed such as clipping and filtering, coding, SLM, PTS, TR, and so on. Each scheme has its own characteristic and trade-off between the PAPR reduction and other performances of the OFDM system.

In this chapter, we review the conventional PAPR reduction schemes and discuss the related optimization problems as well as the advantages and disadvantages in terms of the PAPR reduction capability, computational complexity, BER degradation, and power increase, etc.

3.1. Clipping and Filtering

A clipping is the simplest technique to reduce high peak value of OFDM signal. This is to clip the OFDM signal deliberately before amplification [22], [23]. The discrete time domain signal clipped at a threshold A is given as

$$\text{clip}_A(x_n) = \begin{cases} -A, & x_n < -A \\ x_n, & -A \le x_n \le A \\ A, & x_n > A \end{cases} \tag{3.1}$$

Table 3.1: Comparison of PAPR reduction schemes.

Method	BER increase	Data rate loss	Complexity	Power increase
Clipping and filtering	yes	no	low	no
Coding	no	high	low	no
SLM	no	low	high	no
PTS	no	low	high	no
TR	no	middle	middle	yes
TI	no	middle	middle	yes
ACE [24]	no	no	high	yes

where x_k is input signal and $\text{clip}_A(x_n)$ denotes its output. Since the OFDM signal with the high peak power rarely occurs, the clipping is an effective method for reducing the PAPR. But, this technique increases the in-band distortion and the out-of-band radiation. Filtering is to eliminate the out-of-band radiation caused from clipping in time domain by using a lowpass filter. However, this technique degrades BER performance due to increment of the in-band distortion of the clipped OFDM signal [22]. While the spectral constraints of the OFDM systems is easily satisfied by clipping and filtering, the degradation of BER performance cannot be acceptable.

3.2. Coding

Coding techniques only transmit the codewords having low PAPR [25]–[28]. To maximize the number of bits transmitted per OFDM symbols, there must be a large number of codewords. However, up to now, all coding techniques have a very small set of possible codewords. Also, exhaustive searches for low PAPR symbols have been required. These methods

exchange low PAPR with the data rate loss. In fact, the computational complexity to search and store these codewords exponentially increase as the number of subcarriers increases. For this reason, it is known that these methods are not practical.

3.3. Selected Mapping

In the SLM scheme, the input symbol sequence is multiplied by each of the U phase sequences to generate alternative symbol sequences. To generate U alternative symbol sequences that include the same information, all elements of $\mathbf{P}^u = [P_0^u \ P_1^u \ \cdots \ P_{N-1}^u]^T$ have the unit magnitude, that is, $P_n^u = e^{j\phi_n^u}$, $\phi_n^u \in [0, 2\pi)$, $0 \leq n \leq N-1, 0 \leq u \leq U-1$. In general, binary or quaternary elements are used for P_k^u, that is, $\{\pm 1\}$ or $\{\pm 1, \pm j\}$. Therefore, alternative symbol sequences $\mathbf{X}^u = [X_0^u \ X_1^u \ \cdots \ X_{N-1}^u]^T, 0 \leq u \leq U-1$ are generated as $\mathbf{X}^u = \mathbf{X} \otimes \mathbf{P}^u$, where $\mathbf{X} \otimes \mathbf{P}^u$ represent the component-wise multiplication of $\mathbf{X}$ and $\mathbf{P}^u$. IFFT is performed for each of U alternative input symbol sequences to generate U alternative OFDM signal sequences, and then the one with the lowest PAPR is selected for transmission. In order to recover the original input symbol sequence in the receiver, the transmitter must send the side information.

3.4. Low-Complexity SLM Schemes

3.4.1. SLM Scheme with Low Complexity

A SLM scheme with low computational complexity is proposed in [29]. The proposed SLM scheme is a technique for applying the SLM scheme to the intermediate stage of IFFT. The key idea of this scheme is that the N point IFFT based on decimation-in-time algorithm is partitioned into two parts, i.e., the first l stages and the remaining $n-l$ stages of IFFT. To generate alternative OFDM signals, the different U phase sequences, $\mathbf{P}^u,\ 1 \leq u \leq U$, is multiplied by the OFDM signal in the intermediate lth stage of IFFT. Since the proposed SLM scheme uses the intermediated stage signals instead of the input symbol sequence, its computational complexity is reduced compared to the conventional SLM scheme.

When the number of subcarriers is $N = 2^n$, the numbers of complex multiplications n_{mul} and complex additions n_{add} of the conventional SLM scheme are given as $n_{\text{mul}} = 2^{n-1}nU$ and $n_{\text{add}} = 2^n nU$, respectively. If the phase sequences are multiplied after the lth stage of IFFT, the numbers of complex computations of the proposed SLM scheme are given as $n_{\text{mul}} = 2^{n-1}n + 2^{n-1}(n-l)(U-1)$ and $n_{\text{add}} = 2^n n + 2^n(n-l)(U-1)$.

When $n-l = 5$, the proposed SLM scheme has almost the same PAPR reduction performance as that of the conventional SLM scheme. Therefore, in the case of $n-l = 5$, the proposed scheme reduces the computational complexity by $41 \sim 51\%$ as U increases from 4 to 16.

3.4.2. SLM Scheme Using Conversion Matrix

In [30]–[32], Wang proposed a new SLM scheme which reduces the computational complexity by substituting the conversion matrix for IFFT. In the proposed SLM scheme, the alternative OFDM signal sequences are generated by multiplying the original OFDM signal sequence by the conversion matrices, where the number of nonzero elements is $4N$ and the nonzero elements belong to the set $\{\pm 1, \pm j\}$. Let $\mathbf{P}^u = \mathrm{diag}(P_1^u, P_2^u, \cdots, P_{N-1}^u)$ be an $N \times N$ diagonal matrix. Then, alternative OFDM signal sequences are given as

$$\mathbf{x}^u = \mathbf{Q}\mathbf{P}^u\mathbf{X} = \mathbf{Q}\mathbf{P}^u\mathbf{Q}^{-1}\mathbf{x} = \mathbf{T}^u\mathbf{x} \tag{3.2}$$

where $\mathbf{T}^u = \mathbf{Q}\mathbf{P}^u\mathbf{Q}^{-1}$ is a conversion matrix. Thus, it is easy to check that the conversion with $\mathbf{T}^u$ requires only $3N$ complex additions.

For example of $N = 16$ and $\mathbf{P}^u = [1\ j\ 1\ -j\ 1\ j\ 1\ -j\ 1\ j\ 1\ -j\ 1\ j\ 1\ -j]^T$, the ith column vector $\mathbf{t}_i^u$ of the conversion matrix $\mathbf{T}^u$ is expressed as

$$\mathbf{t}_i^{(u)} = [1\ 0\ 0\ 0\ -1\ 0\ 0\ 0\ 1\ 0\ 0\ 0\ 1\ 0\ 0\ 0]^T_{((i))},\ 0 \le i \le 15$$

where $[\cdot]_{((i))}$ is a circularly down-shifted version of column vector $[\cdot]$ by i. Since all the column vectors only have four nonzero elements, the number of nonzero elements of the conversion matrix is 64 $(= 4 \times 16)$.

It is worth mentioning that the phase vector must have periodicity in order to maintain $4N$ nonzero elements of the conversion matrix and this

leads to the degradation of the PAPR reduction performance.

3.5. Partial Transmit Sequence

In the conventional PTS scheme, an input signal sequence $\mathbf{X}$ is partitioned into V disjoint symbol subsequences $\mathbf{X}_v = [X_{v,0}\ X_{v,1}\ \cdots\ X_{v,N-1}]$, $0 \le v \le V-1$, which can be expressed by

$$\mathbf{X} = \sum_{v=0}^{V-1} \mathbf{X}_v. \tag{3.3}$$

For each symbol subsequence, $X_{v,k} = 0$, $0 \le k \le N-1$, except for N/V data symbols. The signal subsequence $\mathbf{x}_v = [x_{v,0}\ x_{v,1}\ \cdots\ x_{v,N-1}]$, called a subblock, is generated by applying IFFT to each symbol subsequence $\mathbf{X}_v$. Each subblock $\mathbf{x}_v$ is multiplied by a rotating factor b_v^u with an unit magnitude selected from a given alphabet set $\mathbb{B}$, which is usually $\mathbb{B} = \{\pm 1\}$ or $\mathbb{B} = \{\pm 1, \pm j\}$. From the sum of the subblocks multiplied by b_v^u, the uth alternative signal sequence $\mathbf{x}^u = [x_0^u\ x_1^u\ \cdots\ x_{N-1}^u]$ can be obtained by

$$\mathbf{x}^u = \sum_{v=0}^{V-1} b_v^u \mathbf{x}_v \tag{3.4}$$

where $0 \le u \le U-1$ and $U = |\mathbb{B}|^{V-1}$. Let $\mathbf{b}^u = [b_0^u\ b_1^u\ \cdots\ b_{V-1}^u]$ be the uth rotating vector, where $\mathbf{b}^u \in \mathbb{B}^V$. In order to choose the alternative signal sequence with the minimum PAPR for transmission, the optimized

rotating vector $\mathbf{b}^{\tilde{u}} = \left[b_0^{\tilde{u}}\ b_1^{\tilde{u}}\ \cdots\ b_{V-1}^{\tilde{u}}\right]$ can be obtained by

$$\mathbf{b}^{\tilde{u}} = \arg\min_{\mathbf{b}^u \in \mathbb{B}^V} \left(\max_{0 \le n \le N-1} \left| \sum_{v=0}^{V-1} b_v x_{v,n} \right| \right). \tag{3.5}$$

The PAPR reduction performance depends on the method of subblock partitioning. The subblock partitioning methods such as adjacent, interleaving, and random subblock partitioning exist. It is well known that the random subblock partitioning has the best performance for the PAPR reduction.

In the PTS scheme, the transmitter is required to send the SI of rotating vector $\mathbf{b}^{\tilde{u}}$ to recover the original symbol sequence in the receiver. The BER performance in OFDM systems is critically degraded when detection of the SI is failed. Since the SI is usually encoded for error detection and correction due to its importance, it degrades the spectrum efficiency.

In [33], a PTS scheme with low complexity was proposed for reducing the computational complexity of IFFTs. Unlike the conventional PTS scheme, where input symbol sequences are partitioned at the initial stage, the proposed PTS scheme performs block partitioning after the first l stages of IFFT. In this scheme, the 2^n-point IFFT based on the decimation-in-time algorithm is divided into two parts. The first part is the first l stages and the second part is the remaining $n - l$ stages of IFFT. In the first l stages of IFFT, the input symbol sequence $\mathbf{X}$ is partially IFFTed to form an intermediate signal sequence $\hat{\mathbf{x}}^l$. This intermediate signal sequence is partitioned into V intermediate signal subsequences and then,

the remaining $n-l$ stages of IFFT are applied to each of the intermediate signal subsequences.

Compared to the conventional PTS scheme, the computational complexity of the proposed PTS scheme is lower, because there is a common intermediate signal sequence $\hat{\mathbf{x}}^l$ for IFFT of V symbol subsequences. When the number of subcarriers is $N = 2^n$, the numbers of complex multiplications n_{mul} and complex additions n_{add} of the conventional PTS scheme are given as $n_{\text{mul}} = 2^{n-1}nV$ and $n_{\text{add}} = 2^n nV$, respectively, where V is the number of subblocks. If the intermediate signal is partitioned after the lth stage of IFFT, it is clear that the numbers of complex computations of the proposed PTS scheme are given as $n_{\text{mul}} = 2^{n-1}n + 2^{n-l}(n-l)(V-1)$ and $n_{\text{add}} = 2^n n + 2^n(n-l)(V-1)$.

3.6. Tone Reservation

The TR scheme reserves some tones for generating a PAPR reduction signal instead of data transmission [6]. Let $\mathcal{R} = \{i_1, i_2, \cdots, i_W\}$ denote the ordered set of the positions of the reserved tones and $\mathcal{R}^{\text{c}}$ denote the complement set of $\mathcal{R}$ in $\mathcal{N} = \{0, 1, \cdots, N-1\}$, where W is the numbers of the reserved tones. Then, the input symbol A_k is expressed as

$$X_k = A_k + C_k = \begin{cases} C_k, & k \in \mathcal{R} \\ A_k, & k \in \mathcal{R}^{\text{c}} \end{cases}$$

where A_k is the data symbol with 0 in the set $\mathcal{R}$ and C_k is the PAPR reduction symbol with 0 in the set $\mathcal{R}^{\mathrm{c}}$. Let $x_n,\ a_n$, and c_n be the time domain signals obtained by IFFTing $X_k,\ A_k$, and C_k, respectively. Since IFFT is a linear operation, the baseband discrete time OFDM signal x_n corresponds to the summation of the data signal a_n and the PAPR reduction signal c_n, i.e., $x_n = a_n + c_n$.

Next, we consider the generation method of peak reduction signals. Peak reduction signals are iteratively generated as follows. Let $\mathbf{f} = [f_0\ f_1 \cdots f_{N-1}]^T$ be the time domain kernel signal defined by

$$f_n = \frac{1}{\sqrt{N}} \sum_{k \in \mathcal{R}} F_k e^{j2\pi \frac{k}{N} n}$$

where $\mathbf{F} = [F_0\ F_1\ \cdots\ F_{N-1}]^T$ is PRT set with $F_k = 0$ for $k \in \mathcal{R}^{\mathrm{c}}$. The kernel signal $\mathbf{f}$ is used to compute the PAPR reduction signal sequence $\mathbf{c}$ iteratively [6]. That is, the PAPR reduction signal sequence $\mathbf{c}^l$ at the lth iteration is obtained as

$$\mathbf{c}^l = \sum_{i=1}^{l} \alpha_i \mathbf{f}_{((\tau_i))} \tag{3.6}$$

where $\mathbf{f}_{((\tau_i))}$ denotes a circular shift of $\mathbf{p}$ by τ_i and α_i is a complex scaling factor computed according to the target threshold level γ_{th} and the maximum peak value at the ith iteration. The circular shift τ_i is determined as

$$\tau_i = \underset{0 \le n \le LN-1}{\operatorname{argmax}} |a_n + c_n^{i-1}|.$$

Then, the OFDM signal in the TR scheme at the lth iteration can be represented as

$$\mathbf{x} = \mathbf{a} + \mathbf{c}^l. \tag{3.7}$$

Chapter 4. A New Blind SLM Scheme with Low Decoding Complexity for OFDM Systems

It is well known that SLM scheme can effectively reduce the PAPR of OFDM signals without signal distortion by using symbol scrambling techniques. In the SLM scheme, an input symbol sequence is componentwisely multiplied by each of phase sequences to yield alternative symbol sequences. Then, these alternative symbol sequences are IFFTed and the one with the minimum PAPR is selected for transmission.

However, in the SLM scheme, the SI must be transmitted to allow the recovery of original symbol sequence at the receiver, which reduces the data transmission rate. Also, an erroneous detection of the SI causes a significant influence on the BER. Therefore, strong protection of the side information is required, which cause more loss of data transmission rate. To remove the transmission of such SI, several BSLM schemes have been studied [13]–[15]. Among them, the maximum likelihood (ML) decoder is derived for the BSLM scheme in [15], which shows the same BER performance as the SLM scheme assuming perfect SI but causes large decoding complexity at the receiver.

In this chapter, a new BSLM scheme with low decoding complexity is proposed. In the proposed BSLM scheme, the SI is embedded into each phase sequence by giving the phase offset to the elements of the phase sequence, which is determined by the biorthogonal vectors for the partitioned subblocks. An ML decoder with low decoding complexity is derived for the proposed BSLM scheme, which reduces the decoding complexity by $(U-2)/U$ compared with the conventional BSLM scheme in [15]. The DFP of the SI for the proposed BSLM scheme is derived and the closed-form expression of DFP is obtained for $U = 4$ and 8 over the AWGN channel. Also, PEP analysis for the proposed BSLM scheme is derived over the fading channel. Based on the PEP analysis, BER performance of the proposed BSLM scheme is shown to be determined by subblock partitioning and phase offset. Also, the numerical results show that for the OFDM systems with QPSK and 16-QAM, the DFP and BER of the proposed BSLM scheme are almost the same as those of the conventional BSLM scheme.

The rest of the chapter is organized as follows. First, a conventional BSLM scheme is explained in Section 4.1. In Section 4.2, a new BSLM scheme is proposed and the phase offset and the subblock phase offset vectors to embed the SI into the phase sequence are investigated. The DFP of SI and the PEP for the proposed BSLM scheme is analyzed in Section 4.3 and the numerical results are given to show the performance of the proposed BSLM scheme in Section 4.4. Finally, Section 4.5 concludes this chapter.

4.1. Conventional Blind SLM Scheme

In the conventional SLM scheme, an input symbol sequence $\mathbf{X}$ is componentwisely multiplied by each of U phase sequences to generate U alternative symbol sequences. IFFT is performed to each alternative symbol sequence and the one with the minimum PAPR is transmitted. Suppose that U phase sequences are given as $\mathbf{P}^u = [P_0^u \ P_1^u \ \cdots \ P_{N-1}^u]$, where $P_n^u = e^{j\phi_n^u}$, $\phi_n^u \in [0, 2\pi)$ and $u \in \{1, 2, \cdots, U\}$. Let $\mathbf{a} \otimes \mathbf{b}$ represent the componentwise multiplication of vectors $\mathbf{a}$ and $\mathbf{b}$. For an input symbol sequence $\mathbf{X}$, $\mathbf{x}^{\tilde{u}}$ with the minimum PAPR among $\mathbf{x}^u = \text{IFFT}(\mathbf{X} \otimes \mathbf{P}^u)$, $1 \leq u \leq U$, is selected for transmission. Also, the index $\tilde{u}$ of the selected phase sequence, called SI, should be transmitted to the receiver.

In order to eliminate the transmission of the SI, the BSLM scheme was proposed in [15], where the phase sequences are modified and a simplified ML decoder for the BSLM scheme is proposed. The key idea of the BSLM scheme is to make the Euclidean distances among U phase sequences large. By using such phase sequences and ML decoder, the BSLM scheme enables a receiver to recover the input symbol sequence without using SI.

Suppose that the received signal sequence is $\mathbf{r} = \mathbf{x}^{\tilde{u}} + \mathbf{n}$, where $\mathbf{r} = [r_0 \ r_1 \ \cdots \ r_{N-1}]$ and $\mathbf{n} = [n_0 \ n_1 \ \cdots \ n_{N-1}]$ is a noise sequence in the time domain. Then, the received symbol sequence $\mathbf{R} = [R_0 \ R_1 \ \cdots \ R_{N-1}]$ is obtained by FFTing $\mathbf{r}$. In order to correctly decode $\mathbf{R}$ in the conventional BSLM scheme, U phase sequences should have the following properties:

- The set of phase sequences $\mathbf{P}^u$ is fixed and known a priori;

- $\mathbf{X} \otimes \mathbf{P}^u$ and $\mathbf{X} \otimes \mathbf{P}^v$ are sufficiently different for any input symbol sequence $\mathbf{X}$ when $u \neq v$.

In order for the decoder of the conventional BSLM scheme to work well, each phase ϕ_n^u of $\mathbf{P}^u$ for all n and u must satisfy the condition $X_n e^{j\phi_n^u} \notin \mathcal{Q}$ and the set of $\mathbf{P}^u$ should be chosen to ensure the condition in [15]. Further, if $u \neq \tilde{u}$ and the channel noise is not considered, each element of $\mathbf{R} \otimes \mathbf{P}^{u*}$ should not be contained in the constellation $\mathcal{Q}$, where $\mathbf{P}^{u*}$ is the complex conjugate of $\mathbf{P}^u$. Based on these properties, a simplified ML decoder for the conventional BSLM scheme was derived to recover the data symbols without knowing the SI [15]. Clearly, if the Euclidean distance between any $\mathbf{P}^u$ and $\mathbf{P}^v$ is large enough, the BER performance of this ML decoder is expected to be good.

The received symbol R_n after performing FFT demodulation at the receiver can be written as

$$R_n = G_n X_n e^{j\phi_n^{\tilde{u}}} + N_n \tag{4.1}$$

where G_n is the frequency response of the fading channel at the nth subcarrier and N_n is an AWGN sample at the nth subcarrier. We assume that the channel is a quasi static Rayleigh fading channel and G_n is independent and perfectly known at the receiver, i.e., the perfect channel state information (CSI) is assumed. Under these assumptions, the ML decoder computes the decision metric to decode the received symbol sequence $\mathbf{R}$

without knowing the SI $\tilde{u}$ [15] given as

$$D_{BSLM} = \min_{\mathbf{P}^u, u\in\{1,2,\cdots,U\}} \sum_{n=0}^{N-1} \min_{X'_n\in\mathcal{Q}} |R_n e^{-j\phi_n^u} - \hat{G}_n X'_n|^2 \tag{4.2}$$

where $|\cdot|$ denotes the absolute value of a complex number and $\hat{G}_n$ is the estimated channel response. This decoding is explained in detail as follows. Let $\hat{X}_n^u$ be the constellation point in $\mathcal{Q}$, which minimizes the Euclidean distance between $R_n e^{-j\phi_n^u}$ and $\hat{G}_n X'_n$. For each subcarrier n and P_n^u, $\hat{X}_n^u$ is obtained and its metric $|R_n e^{-j\phi_n^u} - \hat{G}_n \hat{X}_n^u|^2$ is stored. Then, the minimum metrics for all subcarriers are summed for the given $\mathbf{P}^u$. This process is repeated for each phase sequence $\mathbf{P}^u$, $1 \le u \le U$. Finally, the input symbol sequence is recovered from the decoded symbol sequence $\hat{\mathbf{X}}^{\hat{u}} = [\hat{X}_0^{\hat{u}}\ \hat{X}_1^{\hat{u}} \cdots \hat{X}_{N-1}^{\hat{u}}]$ with the minimum decision metric D_{BSLM}.

Consequently, the overall decoding complexity to find D_{BSLM} in (4.2) is UqN $|\cdot|^2$ operations if the real additions are ignored because the complexity of $|\cdot|^2$ operation is much larger than that of real addition. Since the decoder in (4.2) is still complicated, a new BSLM scheme with low decoding complexity is proposed in the next section.

4.2. New Blind SLM Scheme

4.2.1. Embedding Side Information into Phase Sequences

In the conventional BSLM scheme [15], it is important that ϕ_n^u is uniformly distributed over $[0, 2\pi)$ and satisfies the condition $X_n e^{j\phi_n^u} \notin \mathcal{Q}$.

Under these conditions, phase sequences with large Euclidean distance can be constructed, but the decoding complexity of ML decoder at the receiver is large. Therefore, in order to achieve low decoding complexity at the receiver, we propose a new approach to embed the SI into the phase sequence.

Instead of randomly selecting each phase ϕ_n^u for U phase sequences, we choose P_n^u $(= e^{j\phi_n^u})$ from $\{+1, -1\}$ or $\{\pm 1, \pm j\}$ to keep the original signal constellation $\mathcal{Q}$. It is well known that if P_n^u is uniformly distributed over $\{+1, -1\}$ or $\{\pm 1, \pm j\}$, the phase sequences are optimal [34], [35]. In order to embed the SI into the phase sequence, we modify the phase sequences by using the block partitioning and giving the phase offset to the signal constellation $\mathcal{Q}$ as follows.

Suppose that U phase sequences are used. The uth phase sequence $\mathbf{P}^u$ is partitioned into L subblocks as $[\mathbf{P}_1^u\ \mathbf{P}_2^u\ \cdots\ \mathbf{P}_L^u]$, where $\mathbf{P}_l^u = [P^u_{\frac{N(l-1)}{L}}\ P^u_{\frac{N(l-1)}{L}+1}\ \cdots\ P^u_{\frac{Nl}{L}-1}]$, $1 \le u \le U$, $1 \le l \le L$, is the lth subblock with the size N/L. Now, we define U subblock phase-offset L-tuple vectors as

$$\mathbf{W}^u = [w_1^u\ w_2^u\ \cdots\ w_L^u] \tag{4.3}$$

where $w_l^u \in \{0, 1\}$, $1 \le u \le U$, $1 \le l \le L$. Then, the SI u is embedded into the uth phase sequence by using $\mathbf{W}^u$ as follows. Each element in the lth subblock $\mathbf{P}_l^u$ of $\mathbf{P}^u$ is multiplied by $e^{j\theta w_l^u}$, where $0 < \theta \le \pi/2$ and $1 \le l \le L$. In other words, all elements of each subblock $\mathbf{P}_l^u$ are rotated by the same amount θw_l^u. Then, the modified uth phase sequence $\bar{\mathbf{P}}^u$ can

be written as

$$\bar{\mathbf{P}}^u = [\mathbf{P}_1^u e^{j\theta w_1^u}\ \mathbf{P}_2^u e^{j\theta w_2^u}\ \cdots\ \mathbf{P}_L^u e^{j\theta w_L^u}]. \tag{4.4}$$

Clearly, the index u is embedded into $\bar{\mathbf{P}}^u$ by the subblock phase-offset L-tuple vector $\mathbf{W}^u$ by using all distinct subblock phase-offset L-tuple vectors $\mathbf{W}^u$, $1 \le u \le U$. The transmitter uses the modified phase sequences $\bar{\mathbf{P}}^u$ for PAPR reduction of OFDM signals. Thus, it is equivalent to use two signal constellations such that each element in the subblock with $w_l^u = 0$ is modulated by using the signal constellation $\mathcal{Q}$ and each element in the subblock with $w_l^u = 1$ is modulated by using the signal constellation $\mathcal{Q}_\theta$, which is obtained by rotating the $\mathcal{Q}$ by θ.

4.2.2. ML Decoding Algorithm at the Receiver

From the received signal with the modified phase sequence $\bar{\mathbf{P}}^{\tilde{u}}$, the receiver should find the index $\tilde{u}$ without any SI and recover the input symbol sequence $\mathbf{X}$. In this subsection, an ML decoder with low decoding complexity is proposed as follows. The received symbol sequence $\mathbf{R}$ is partitioned into L subblocks as $[\mathbf{R}_1\ \mathbf{R}_2 \cdots \mathbf{R}_L]$, where $\mathbf{R}_l = [R_{\frac{N(l-1)}{L}}\ R_{\frac{N(l-1)}{L}+1} \cdots R_{\frac{Nl}{L}-1}]$, $1 \le l \le L$. The ML decoder without SI at the receiver is operated in two steps. First, the metric for each received subblock $\mathbf{R}_l$ is calculated as

$$D_{l,p} = \sum_{n=\frac{N(l-1)}{L}}^{\frac{Nl}{L}-1} \min_{X'_n \in \mathcal{Q}} |R_n e^{-j\theta p} - \hat{G}_n X'_n|^2 \tag{4.5}$$

where $p \in \{0,1\}$ and $1 \le l \le L$. The decoder in (4.5) is operated as the ML decoding process for the conventional BSLM scheme. Let $\hat{X}_n^p$ be the constellation point in $\mathcal{Q}$, which minimizes the Euclidean distance between $R_n e^{-j\theta_p}$ and $\hat{G}_n X'_n$. For the lth subblock and given p, $\hat{X}_n^p$ for each subcarrier in the subblock is obtained and its metric $|R_n e^{-j\theta_p} - \hat{G}_n \hat{X}_n^p|^2$ is added to $D_{l,p}$. Then, we obtain $D_{l,0}$ and $D_{l,1}$, and also the decoded subblocks $\hat{\mathbf{X}}_l^0$ and $\hat{\mathbf{X}}_l^1$, where $\hat{\mathbf{X}}_l^p = [\hat{X}^p_{\frac{N(l-1)}{L}} \ \hat{X}^p_{\frac{N(l-1)}{L}+1} \ \cdots \ \hat{X}^p_{\frac{Nl}{L}-1}]$. This process is repeated for all l, $1 \le l \le L$.

Finally, the ML decoder finds $\hat{u}$ with the minimum value $D_{\hat{u}}$ among U sum values D_u corresponding to $\mathbf{W}^u$ as

$$\hat{u} = \arg\min_{1 \le u \le U} D_u = \arg\min_{1 \le u \le U} \sum_{l=1}^{L} D_{l,w_l^u}. \tag{4.6}$$

By using $\mathbf{W}^{\hat{u}}$ corresponding to the index $\hat{u}$ in (4.6), the decoded symbol sequence $\hat{\mathbf{X}}^{\hat{u}} = [\hat{\mathbf{X}}_1^{w_1^{\hat{u}}} \ \hat{\mathbf{X}}_2^{w_2^{\hat{u}}} \ \cdots \ \hat{\mathbf{X}}_L^{w_L^{\hat{u}}}]$ is obtained, where the phase offset $\theta w_l^{\hat{u}}$ from each decoded subblock $\mathbf{R}_l$ is already removed, that is, $\hat{\mathbf{X}}^{\hat{u}} = \hat{\mathbf{X}} \otimes \mathbf{P}^{\hat{u}}$. Since (4.5) and (4.6) decode $\mathbf{R}$ and only eliminate the phase offset $[e^{j\theta w_1^{\hat{u}}} \ e^{j\theta w_2^{\hat{u}}} \ \cdots \ e^{j\theta w_L^{\hat{u}}}]$ from $\mathbf{R}$, the input symbol sequence is determined by $\hat{\mathbf{X}}^{\hat{u}} \otimes \mathbf{P}^{\hat{u}*}$. In conclusion, while the ML decoder for the conventional BSLM scheme finds the phase sequence, the ML decoder for the proposed BSLM scheme finds the used subblock phase-offset L-tuple vector $\mathbf{W}^u$ by using D_u in (4.6).

The total decoding complexity of the proposed BSLM scheme to find the index $\hat{u}$ and the decoded symbol sequence $\hat{\mathbf{X}}^{\hat{u}}$ in (4.5) and (4.6) is only

$2qN$ $|\cdot|^2$ operations if the real additions are ignored as in the conventional BSLM scheme.

4.2.3. Optimal Subblock Phase-Offset L-Tuple Vectors $\mathbf{W}^u$ and Phase Offset θ

In this subsection, we derive the optimal θ and construct the optimal U subblock phase-offset L-tuple vectors $\mathbf{W}^u$ which maximize the detection probability of the SI at the receiver. First, we propose the design criterion for $\mathbf{W}^u$ as:

- Let $d_{\min}$ be the minimum Hamming distance between $\mathbf{W}^u$'s. Then, the normalized minimum Hamming distance $d_{\min}/L$ should be maximized for given U.

The reason for the design criterion for the subblock phase-offset L-tuple vectors is explained as follows. The proposed ML decoder should extract the SI from the received symbol sequence $\mathbf{R}$. In order to minimize the DFP of the SI in (4.6), the minimum difference between $D_{\tilde{u}}$ and D_v for given $\mathbf{R}$, $\tilde{u} \neq v$, should be as large as possible. Clearly, the number of subblocks to decide the minimum difference between $D_{\tilde{u}}$ and D_v, $\tilde{u} \neq v$, is $d_{\min}$. The metric (4.5) for each received subblock $\mathbf{R}_l$ is calculated by N/L sums of $\min_{X'_n \in \mathcal{Q}} |R_n e^{-j\theta p} - \hat{G}_n X'_n|^2$. Then, we can expect that the minimum difference between $D_{\tilde{u}}$ and D_v, $\tilde{u} \neq v$, in (4.6) is determined by $d_{\min}N/L$ sums of $\min_{X'_n \in \mathcal{Q}} |R_n e^{-j\theta p} - \hat{G}_n X'_n|^2$. Thus, for given N and U, the normalized minimum Hamming distance $d_{\min}/L$ of the set of U subblock phase-offset L-tuple vectors should be maximized.

It is well known that the following sets of binary vectors have large $d_{\min}/L$ [36]: A set of biorthogonal vectors, a set of orthogonal vectors, and a set of binary vectors constructed by simplex code (e.g., m-sequence). A set of binary vectors constructed by simplex code have the largest $d_{\min}/L = L/\{2(L-1)\}$ while the other two vector sets have $d_{\min}/L = 0.5$. However, the size of subblock may not be well expressed from its odd length $2^k - 1$ simplex codes. Therefore, we propose U biorthogonal vectors of length L as the best subblock phase-offset L-tuple vectors $\mathbf{W}^u$, $1 \leq u \leq U$, which give us the slightly better performance than the orthogonal vectors. The set of the best U subblock phase-offset L-tuple vector $\mathbf{W}^u$'s can be constructed by the biorthogonal vector of length $L = U/2$, where $d_{\min}/L = 0.5$. Fig. 4.1 shows U biorthogonal vectors of length $L = U/2$ for $U = 4$ and 8, which are used as subblock phase-offset L-tuple vectors.

For example, construct a set of 8 subblock phase-offset L-tuple vectors for $U = 8$ as follows: (a) a set of biorthogonal vectors of length $L = U/2 = 4$; (b) a set of binary vectors of length $L = 15$ constructed by simplex code; (c) a set of all vectors of length $L = 3$. Clearly, $d_{\min}/L = 0.5$ for (a), $d_{\min}/L = 8/15$ for (b), and $d_{\min}/L = 1/3$ for (c). Since (b) has the largest $d_{\min}/L$ among them, (b) is the best one among three candidates. However, the DFP performance of (a) as our proposed set for $\mathbf{W}^u$ is almost the same as that of (b). Fig. 4.2 compares the DFP performance of three cases with QPSK, $N = 64$, and $\theta = \pi/4$.

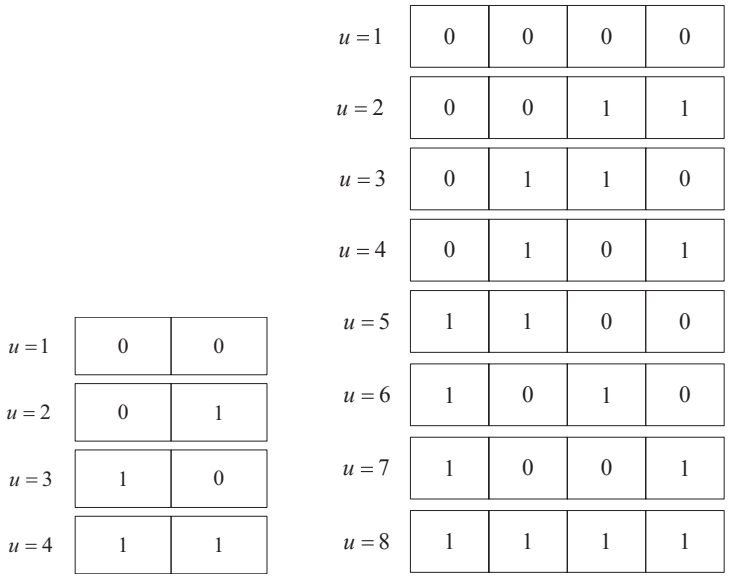

Figure 4.1: Biorthogonal subblock phase-offset L-tuple vectors: (a) $U = 4$ and (b) $U = 8$.

Also, the phase offset value θ must be chosen such that the difference between two constellations $\mathcal{Q}$ and $\mathcal{Q}_\theta$ is maximized to give good detection performance. To do that, an optimal $\tilde{\theta}$ can be selected by

$$\tilde{\theta} = \arg \max_{0<\theta\leq\frac{\pi}{2}} \sum_{X\in\mathcal{Q}} \min_{Y\in\mathcal{Q}_\theta} |X - Y|^2. \tag{4.7}$$

It is easy to check that for QPSK, the optimum $\tilde{\theta}$ is $\pi/4$. Also, by exhaustive search, it is found that the optimal $\tilde{\theta}$ for 16-QAM and 64-QAM is also $\pi/4$. Fig. 4.3 shows the signal constellations $\mathcal{Q}$ and $\mathcal{Q}_{\frac{\pi}{4}}$ for QPSK and 16-QAM. And, Fig. 4.4 compares the DFP performance of various θ in OFDM systems with 16-QAM, $U = 16$, and $N = 64$. It is shown that

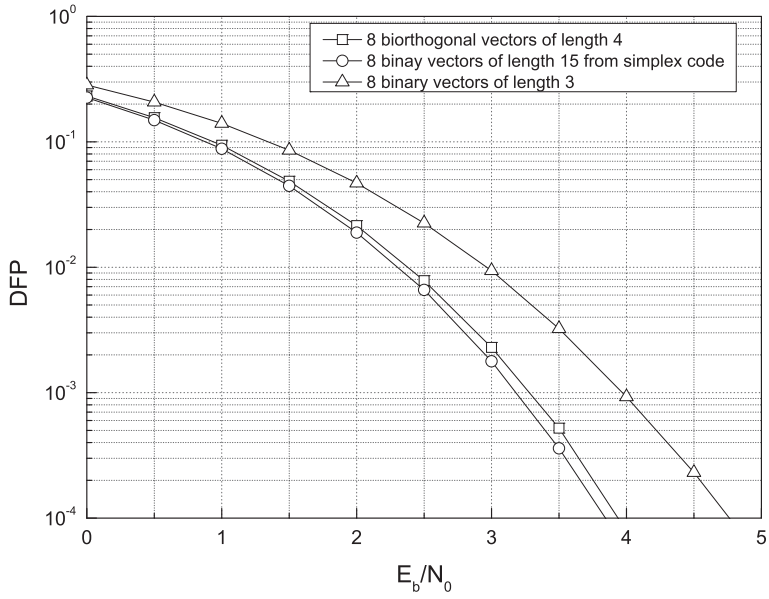

Figure 4.2: Comparison of DFP performance for various subblock phase-offset L-tuple vectors in the OFDM system with QPSK, $N = 256$, $U = 8$, and $\theta = \pi/4$.

the optimal θ is $\pi/4$.

4.2.4. New BSLM Scheme with Low Decoding Complexity

Based on the results in the previous subsections, we propose a new BSLM scheme with low decoding complexity as follows. To embed the SI into the phase sequences, a set of U biorthogonal vectors with $L = U/2$ is used as subblock phase-offset L-tuple vectors and the phase offset $\theta = \pi/4$ is used. The phase sequences are modified by using the block partitioning and giving the phase offset to the signal constellation $\mathcal{Q}$. At the transmitter of the new BSLM scheme, U alternative symbol sequences are generated by modified phase sequences $\bar{\mathbf{P}}^u$, $1 \leq u \leq U$, and the one with

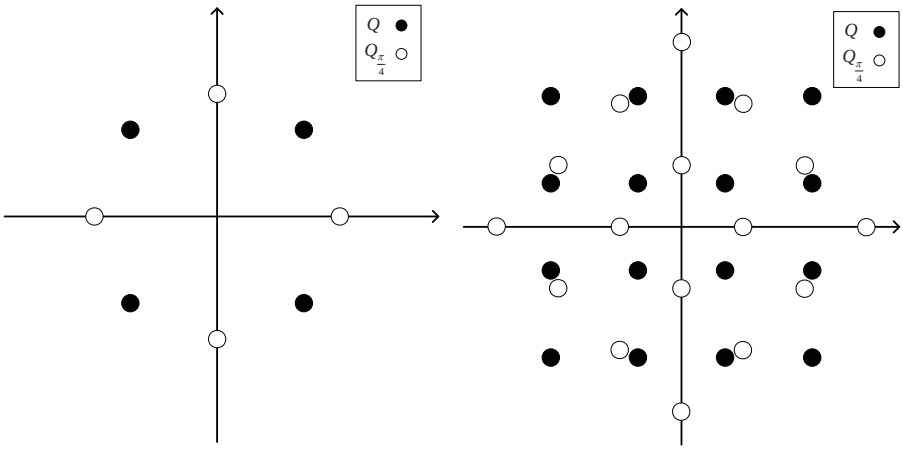

(a) (b)

Figure 4.3: Signal constellations $\mathcal{Q}$ and $\mathcal{Q}_{\frac{\pi}{4}}$: (a) QPSK and (b) 16-QAM.

the minimum PAPR is selected for transmission. From the ML decoder using the decision metrics (4.5) and (4.6) at the receiver, the proposed BSLM scheme can extract the SI from the selected phase sequence and recover the alternative symbol sequence. Fig. 4.5 shows a block diagram of the ML decoder for the proposed BSLM scheme.

It is clear that regardless of U, total complexity of the ML decoder for the proposed BSLM scheme is $2qN$ $|\cdot|^2$ operations when q-ary modulation is used but the decoding complexity of the conventional BSLM scheme is UqN $|\cdot|^2$ operations. Therefore, the decoding complexity reduction ratio (DCRR) of the proposed BSLM scheme over the conventional BSLM

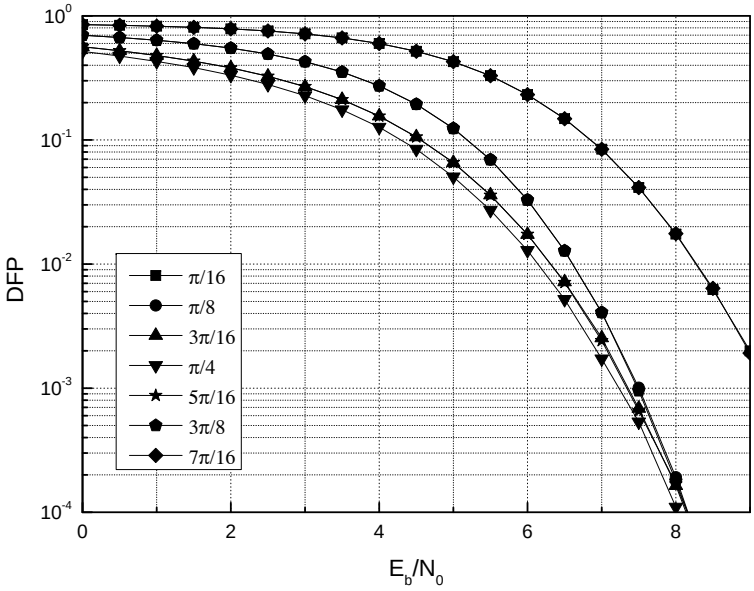

Figure 4.4: Comparison of DFP performance for various θ in the OFDM system with 16-QAM, $N = 64$, and $U = 16$.

scheme in (4.2) is obtained as

$$\begin{aligned} \text{DCRR} &= \left(1 - \frac{\text{Complexity of the proposed BSLM}}{\text{Complexity of the conventional BSLM}}\right) \times 100 \\ &= \left(\frac{UqN - 2qN}{UqN}\right) \times 100 \\ &= \left(\frac{U-2}{U}\right) \times 100 \quad (\%). \end{aligned} \tag{4.8}$$

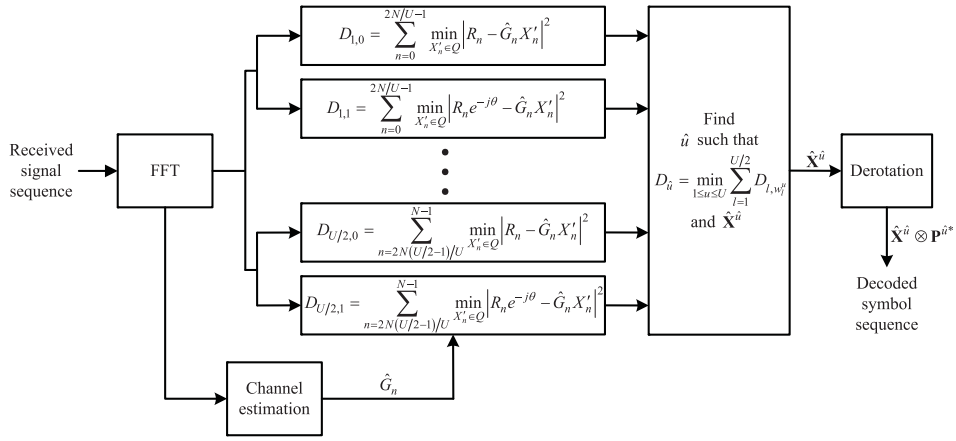

Figure 4.5: A block diagram of the receiver for the proposed BSLM scheme.

4.3. Performance Analysis

4.3.1. DFP Performance of Side Information in AWGN

It is well known that the BER P_e at the receiver for the OFDM system using BSLM scheme is given as

$$P_e = P_b(1 - P_{df}) + P_{b|df} P_{df} \tag{4.9}$$

where P_b is the BER of the OFDM signal, $P_{b|df}$ is the BER when the detection of the SI is failed, and P_{df} is the DFP of the SI [14]. When the detection of the SI is failed, $P_{b|df} = 0.5$. Thus, the detection failure of the side information in the BSLM scheme can seriously deteriorate the BER of the OFDM system. Therefore, analysis of DFP of the embedded SI in the proposed BSLM scheme is very important. In this section, we will

analyze the DFP for the proposed BSLM scheme in the AWGN channel when $U = 4$ and 8 by considering U biorthogonal vectors as the subblock phase offset L-tuple vectors. It will be shown that the decision metrics for the ML decoder of the proposed BSLM scheme in (4.5) and (4.6) work well over the AWGN channel.

In order to analyze the DFP, we can assume that all elements of an input symbol sequence $\mathbf{X}$ are from $\mathcal{Q}$ and the alternative symbol sequence with the minimum PAPR, which is not phase rotated, is selected for transmission. That is, all subcarriers of the OFDM signal are loaded with the symbols from $\mathcal{Q}$ and the selected subblock phase offset vector is all-0 vector $\mathbf{W}^1$. Also, biorthogonal vectors with length $U/2$ are used as the subblock phase offset L-tuple vectors $\mathbf{W}^u$.

Since the correct decision metric value for the transmitted signal is D_1, the detection success probability P_{ds} can be expressed as

$$\begin{aligned} P_{ds} &= \Pr(D_1 < D_2, D_1 < D_3, \cdots, D_1 < D_U) \\ &= \Pr(D_1 - D_2 < 0, D_1 - D_3 < 0, \cdots, D_1 - D_U < 0). \end{aligned} \tag{4.10}$$

Since $D_{l,0} - D_{l,1}$ for $w_l^i = 0$ is not added to $D_1 - D_i$ and $D_{l,0} - D_{l,1}$ for $w_l^i = 1$ is added to $D_1 - D_i$, it is not difficult to derive

$$D_1 - D_i = \sum_{l=1}^{U/2} w_l^i (D_{l,0} - D_{l,1}), \quad 2 \le i \le U \tag{4.11}$$

where $w_v^i \in \{0,1\}$. Therefore, (4.10) can be rewritten as

$$P_{ds} = \Pr\left(\sum_{l=1}^{U/2} w_l^2(D_{l,0} - D_{l,1}) < 0, \sum_{l=1}^{U/2} w_l^3(D_{l,0} - D_{l,1}) < 0, \cdots, \sum_{l=1}^{U/2} w_l^U(D_{l,0} - D_{l,1}) < 0\right). \tag{4.12}$$

Let $\mathbf{W}^j = (\mathbf{W}^i)'$, where $1 \leq i \neq j \leq U$ and $(\cdot)'$ denotes the 1's complement. Note that there always exists $\mathbf{W}^j$ such that $\mathbf{W}^j = (\mathbf{W}^i)'$ because biorthogonal vectors $\mathbf{W}^i$ are considered. Then the last all-1 vector $\mathbf{W}^U$ can be expressed as

$$\mathbf{W}^U = \mathbf{W}^i + \mathbf{W}^j. \tag{4.13}$$

From (4.13), $\sum_{l=1}^{U/2} w_l^U(D_{l,0} - D_{l,1}) < 0$ can be rewritten as

$$\sum_{l=1}^{U/2} w_l^i(D_{l,0} - D_{l,1}) + \sum_{l=1}^{U/2} w_l^j(D_{l,0} - D_{l,1}) < 0. \tag{4.14}$$

Therefore, $\sum_{l=1}^{U/2} w_l^U(D_{l,0} - D_{l,1}) < 0$ can be removed in (4.12).

Let $A_l = D_{l,0} - D_{l,1}$, $1 \leq l \leq U/2$. Then from (4.12), the DFP P_{df} can be expressed as

$$\begin{aligned} P_{df} &= 1 - P_{ds} \\ &= 1 - \Pr\left(\sum_{l=1}^{U/2} w_l^2 A_l < 0, \sum_{l=1}^{U/2} w_l^3 A_l < 0, \cdots, \sum_{l=1}^{U/2} w_l^{U-1} A_l < 0\right). \end{aligned} \tag{4.15}$$

Since it is too complex to derive P_{df} for the general U, we will derive P_{df} for two cases of $U = 4$ and 8. A_v's are statistically independent because of the orthogonality between subcarriers. Therefore, the P_{df}'s for $U = 4$ and 8 from (4.15) and Fig. 4.1 can be obtained by

$$\begin{aligned} P_{df,U=4} &= 1 - \Pr(A_1 < 0, A_2 < 0) \\ &= 1 - \{\Pr(A_1 < 0)\}^2, \qquad \text{for } U = 4. \end{aligned} \tag{4.16}$$

$$\begin{aligned} P_{df,U=8} &= 1 - \Pr(A_1 + A_2 < 0, A_1 + A_3 < 0, A_1 + A_4 < 0, \\ &\quad A_2 + A_3 < 0, A_2 + A_4 < 0, A_3 + A_4 < 0) \\ &= 1 - \Pr(A_1 < 0, A_2 < 0, A_3 < 0, A_4 < 0) \\ &\quad - \sum_{i=1}^{4} \Pr(A_i > 0, A_j < -A_i, \forall j, 1 \le j \ne i \le 4) \\ &= 1 - \{\Pr(A_1 < 0)\}^4 \\ &\quad - 4\Pr(A_1 > 0, A_2 < -A_1, A_3 < -A_1, A_4 < -A_1) \\ &= 1 - \{\Pr(A_1 < 0)\}^4 \\ &\quad - 4\int_0^\infty \Pr(A_1 = a)\Pr(A_2 < -a, A_3 < -a, A_4 < -a)\, da \\ &= 1 - \{\Pr(A_1 < 0)\}^4 \\ &\quad - 4\int_0^\infty \Pr(A_1 = a)\Pr(A_2 < -a)^3\, da, \qquad \text{for } U = 8. \end{aligned} \tag{4.17}$$

For $U > 8$, the DFP can be similarly derived as those for $U = 4$ and 8.

To calculate P_{df} in (4.16) and (4.17), we should know the probability distribution of A_l. $D_{l,0}$ and $D_{l,1}$ are the summation of $|R_n e^{-j\theta w_l^u} -$

$\hat{G}_n\hat{X}_n^p|^2$'s, which are statistically independent random variables. Also, both $D_{l,0}$ and $D_{l,1}$ can be regarded as Gaussian distributed random variables for large N by the central limit theorem. Therefore, A_l is also Gaussian distributed. $\Pr(A_l < 0)$ can be expressed as $\Pr(A_l < 0) = Q(E\{A_l\}/\sigma_{A_l})$, where $1 \leq l \leq L$ and $Q(\cdot)$ is the Q-function. Since $\Pr(A_l = a)$ is the Gaussian probability density function (PDF), $\Pr(A_l = a) = \frac{1}{\sqrt{2\pi}\sigma_{A_l}}\exp\left(-\frac{(a-E\{A_l\})^2}{2\sigma_{A_l}}\right)$. However, it is not easy to calculate the mean and variance of A_l and thus, its mean and variance can be obtained through numerical analysis. After finding the mean and variance of A_l by numerical analysis, the DFPs in (4.16) for $U = 4$ and (4.17) for $U = 8$ can be calculated as

$$P_{df,U=4} = 1 - Q\left(\frac{E\{A_1\}}{\sigma_{A_1}}\right)^2 \tag{4.18}$$

$$P_{df,U=8} = 1 - Q\left(\frac{E\{A_1\}}{\sigma_{A_1}}\right)^4 - 4\int_0^\infty \frac{1}{\sqrt{2\pi}\sigma_{A_1}}\exp\left(-\frac{(a-E\{A_1\})^2}{2\sigma_{A_1}}\right) \cdot Q\left(\frac{a+E\{A_1\}}{\sigma_{A_1}}\right)^3 da. \tag{4.19}$$

Fig. 4.6 compares the theoretical results in (4.18) and (4.19) with the simulation results of DFP when $U = 4$ and 8. It shows that the theoretical results are quite well matched to the simulation results for the proposed BSLM scheme and as N increases, the DFP in the low SNR region becomes negligible.

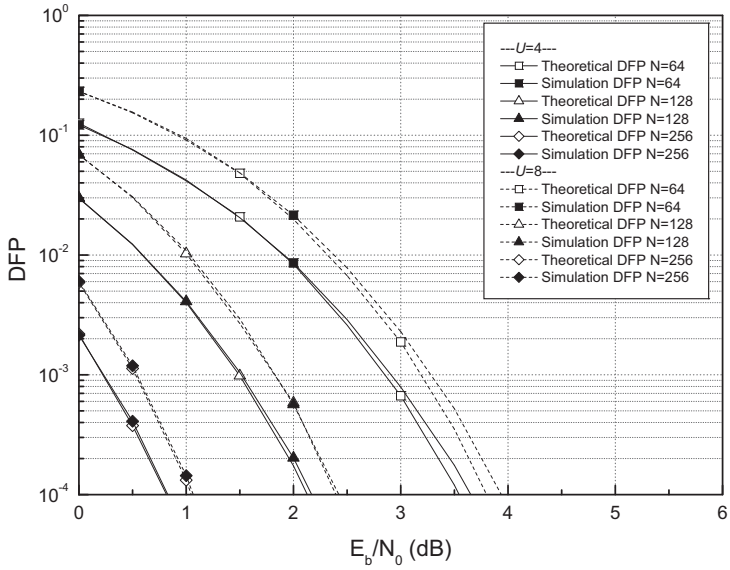

Figure 4.6: Comparison of theoretical and simulated DFPs of the proposed BSLM scheme with $U = 4$ and 8 for QPSK.

4.3.2. BER Performance in Rayleigh Fading Channel

In this subsection, the BER performance of the ML decoder using the decision metrics (4.5) and (4.6) of the proposed BSLM scheme is analyzed. We will derive the PEP, which is the probability to determine $\hat{\mathbf{X}} \otimes \bar{\mathbf{P}}^{\hat{u}}$ when $\mathbf{X} \otimes \bar{\mathbf{P}}^{\tilde{u}}$ is transmitted. In order to analyze the BER performance of communication systems with coding schemes such as trellis codes and space-time codes, PEP approach is widely used. And thus, based on the PEP analysis of the proposed BSLM scheme, we will show that the proposed criteria for subblock phase-offset L-tuple vector and phase offset in the previous section are well behaved.

Assume that the channel is modeled as the Rayleigh fading channel, that is, the coefficients $\hat{G}_n$ are independent samples of complex Gaus-

sian random variables with zero mean and variance 0.5 per dimension. We consider that each element of the signal constellation is contracted by a scale factor $\sqrt{E_s}$ so that the average energy of the constellation elements is 1, where E_s denotes the average energy of the signal constellation points in $\mathcal{Q}$. Therefore, PEP analysis for the proposed BSLM scheme is not dependent upon signal constellations such as QPSK and 16-QAM. Since perfect CSI is assumed, the probability of transmitting $\mathbf{X} \otimes \bar{\mathbf{P}}^{\tilde{u}}$ and deciding $\hat{\mathbf{X}} \otimes \bar{\mathbf{P}}^{\hat{u}}$ at the decoder is well approximated as [37]

$$\begin{aligned} &\Pr\left(\mathbf{X} \otimes \bar{\mathbf{P}}^{\tilde{u}} \to \hat{\mathbf{X}} \otimes \bar{\mathbf{P}}^{\hat{u}} | \hat{G}_n, i = 0, 1, \cdots, N-1\right) \\ &\quad \leq \exp\left(-\frac{d^2(\mathbf{X} \otimes \bar{\mathbf{P}}^{\tilde{u}}, \hat{\mathbf{X}} \otimes \bar{\mathbf{P}}^{\hat{u}}) E_s}{4N_0}\right) \end{aligned} \tag{4.20}$$

where $N_0/2$ is the noise variance per dimension and

$$d^2(\mathbf{X} \otimes \bar{\mathbf{P}}^{\tilde{u}}, \hat{\mathbf{X}} \otimes \bar{\mathbf{P}}^{\hat{u}}) = \sum_{l=1}^{L} \sum_{n=\frac{N(l-1)}{L}}^{\frac{Nl}{L}-1} \left| \hat{G}_n \left(X_n P_n^{\tilde{u}} e^{j\theta w_l^{\tilde{u}}} - \hat{X}_n P_n^{\hat{u}} e^{j\theta w_l^{\hat{u}}} \right) \right|^2.$$

Let $A_n = X_n P_n^{\tilde{u}} e^{j\theta w_l^{\tilde{u}}} - \hat{X}_n P_n^{\hat{u}} e^{j\theta w_l^{\hat{u}}}$, $0 \leq n \leq N-1$, $1 \leq l \leq L$. Since $A_n \neq 0$ for $w_l^{\tilde{u}} \neq w_l^{\hat{u}}$ and $A_n = 0$ for $w_l^{\tilde{u}} = w_l^{\hat{u}}$, the PEP in (4.20) can be modified as

$$\begin{aligned} &\Pr\left(\mathbf{X} \otimes \bar{\mathbf{P}}^{\tilde{u}} \to \hat{\mathbf{X}} \otimes \bar{\mathbf{P}}^{\hat{u}} | \hat{G}_n, i = 0, 1, \cdots, N-1\right) \leq \\ &\qquad \prod_{l \in \mathbb{L}} \prod_{n=\frac{N(l-1)}{L}}^{\frac{Nl}{L}-1} \exp\left(\frac{-|\hat{G}_n A_n|^2 E_s}{4N_0}\right) \end{aligned} \tag{4.21}$$

where $\mathbb{L}$ is a set of l values such that $w_l^{\tilde{u}} \neq w_l^{\hat{u}}$ and the minimum Hamming distance between $\mathbf{W}^{\tilde{u}}$ and $\mathbf{W}^{\hat{u}}$ is $d_{\min}$. Since $\hat{G}_n$ is an independent complex Gaussian random variables with variance 0.5 per dimension and zero mean, $|\hat{G}_n|$'s are independent Rayleigh distributions with PDF

$$\Pr(|\hat{G}_n|) = 2|\hat{G}_n| \exp\left(-|\hat{G}_n|^2\right) \quad \text{for } |\hat{G}_n| \geq 0.$$

Thus, the PEP in (4.21) can be averaged with respect to independent Rayleigh distributions of $|\hat{G}_n|$ as

$$\begin{aligned}\Pr\left(\mathbf{X} \otimes \bar{\mathbf{P}}^{\tilde{u}} \to \hat{\mathbf{X}} \otimes \bar{\mathbf{P}}^{\hat{u}}\right) &\leq \prod_{l \in \mathbb{L}} \left(\frac{1}{\prod_{n=\frac{N(l-1)}{L}}^{\frac{Nl}{L}-1} (1 + |A_n|^2 E_s/4N_0)} \right) \\ &\cong \prod_{l \in \mathbb{L}} \left(\frac{1}{\prod_{n=\frac{N(l-1)}{L}}^{\frac{Nl}{L}-1} (|A_n|^2 E_s/4N_0)} \right). \quad (4.22)\end{aligned}$$

Therefore, from (4.22), the PEP in (4.20) has the following upper bound given as

$$\Pr\left(\mathbf{X} \otimes \bar{\mathbf{P}}^{\tilde{u}} \to \hat{\mathbf{X}} \otimes \bar{\mathbf{P}}^{\hat{u}}\right) \leq \prod_{l \in \mathbb{L}} \left(\prod_{n=\frac{N(l-1)}{L}}^{\frac{Nl}{L}-1} |A_n|^2 \right)^{-1} \left(\frac{E_s}{4N_0}\right)^{-d_{\min}\frac{N}{L}}. \quad (4.23)$$

Note that this is similar to the well-known criteria for the space-time code [37]. In order to decrease error rate in (4.23), it is easy to check that $d_{\min}N/L$ and $|A_n|^2$ should be maximized, respectively. From this results,

it is said that our criteria for the subblock phase-offset L-tuple vector and the phase offset are properly proposed.

4.4. Numerical Results

Simulations for the proposed BSLM scheme with biorthogonal subblock phase-offset L-tuple vectors and phase offset $\theta = \pi/4$ are performed in the OFDM systems modulated by QPSK and 16-QAM. Based on the OFDM systems with $N = 64$ and 256, the simulation results are obtained in the AWGN channel and Rayleigh fading channel. Under $U = 4,\ 8$, and 16, the ML decoding using the metrics (4.5) and (4.6) for the proposed BSLM scheme is performed and compared with the conventional BSLM scheme using the decoding algorithm in (4.2) and the SLM scheme with perfect SI. In order for the decoder of the conventional BSLM scheme to work well, each phase ϕ_n^u of $\mathbf{P}^u$ for all n and u is uniformly distributed over $[0, 2\pi)$ and satisfies the condition $X_n e^{j\phi_n^u} \notin \mathcal{Q}$.

Figs. 4.7 and 4.8 compare the DFP and BER of the proposed and the conventional BSLM schemes with QPSK and 16-QAM in the AWGN channel for various U when $N = 64$ and 256, respectively. For $N = 64$, the DFP performance of the proposed BSLM scheme is better than that of the conventional BSLM scheme for QPSK, but the result is reversed for 16-QAM. However, for 16-QAM, we can see that the DFPs of both BSLM schemes are low enough to give the same BER performance for the practical SNR range achieving the BER $\leq 10^{-2}$. For $N = 256$, the DFP performance of the proposed BSLM scheme is not only better than

that of the conventional BSLM scheme for QPSK but also almost the same as that of the conventional BSLM scheme for 16-QAM. Since the practical OFDM systems usually require the BER less than 10^{-3}, the BER degradation of BSLM scheme due to the DFP of SI in the practical SNR region is negligible.

For QPSK, two constellations in $\mathcal{Q}$ and $\mathcal{Q}_{\frac{\pi}{4}}$ are used for the proposed BSLM scheme. Since rotating phases are randomly selected in the conventional BSLM scheme, rotated symbols may be very close to the symbol in $\mathcal{Q}$, which degrades the performance of the ML decoder of the conventional BSLM scheme in (4.2). Therefore, for QPSK, the DFP of the proposed BSLM scheme is sightly better than that of the conventional BSLM scheme. For 16-QAM, a half of symbols in $\mathcal{Q}_{\frac{\pi}{4}}$ are very close to the symbols in $\mathcal{Q}$ as shown in Fig. 4.3 and hence the performance of ML decoder for the proposed BSLM scheme mostly depends on the other half of symbols. However, since the probability of a rotated symbol being very close to a symbol of $\mathcal{Q}$ is very low in the conventional BSLM scheme, the DFP of the proposed BSLM scheme for 16-QAM is sightly worse than that of the conventional BSLM scheme.

Fig. 4.9 shows the BER performance of the proposed BSLM scheme with $N = 256$ modulated by QPSK and 16-QAM over AWGN channel for a nonlinear HPA with backoff values of 3 and 5 dB. Similar to the BER performance in the AWGN channel, the BER performance of the proposed and the conventional BSLM schemes is exactly matched in the AWGN channel with a nonlinear HPA.

Fig. 4.10 shows the BER performance of the proposed BSLM scheme with $N = 256$, QPSK, and 16-QAM over the Rayleigh fading channel. The decoder of the proposed BLSM scheme performs nearly as good as that of the conventional BSLM scheme in the Rayleigh fading channel.

Fig. 4.11 shows that, for $N = 64$, the proposed BSLM scheme provides almost the same PAPR reduction performance compared with the conventional SLM scheme. Also, for $N = 256$, the PAPR reduction performance of the proposed BSLM scheme is identical to that of the conventional SLM scheme.

4.5. Conclusion

In this chapter, a new BSLM scheme with low decoding complexity is proposed for PAPR reduction of OFDM signals. In the proposed BSLM scheme, the side information is embedded into each phase sequence by giving the phase offset to the elements of phase sequences, which are determined by the biorthogonal vectors for the partitioned subblocks. Also, the proposed BSLM scheme reduces the decoding complexity by $(U-2)/U$ compared with the conventional BSLM scheme. The numerical results show that for QPSK and 16-QAM, the BER and the PAPR reduction performance of the proposed BSLM scheme are almost the same as those of the conventional BSLM scheme. Due to the reduced decoding complexity, the proposed BSLM scheme is practically better than the conventional BSLM scheme, especially for the high data rate OFDM systems.

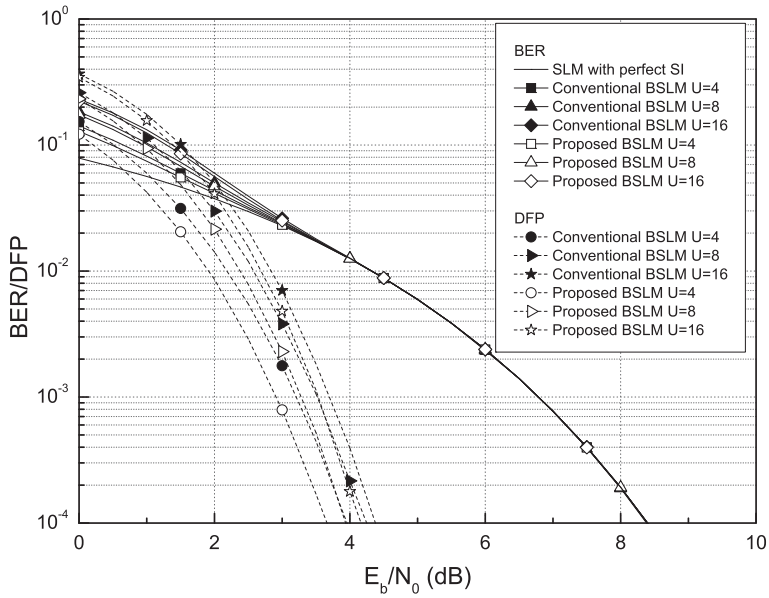

(a)

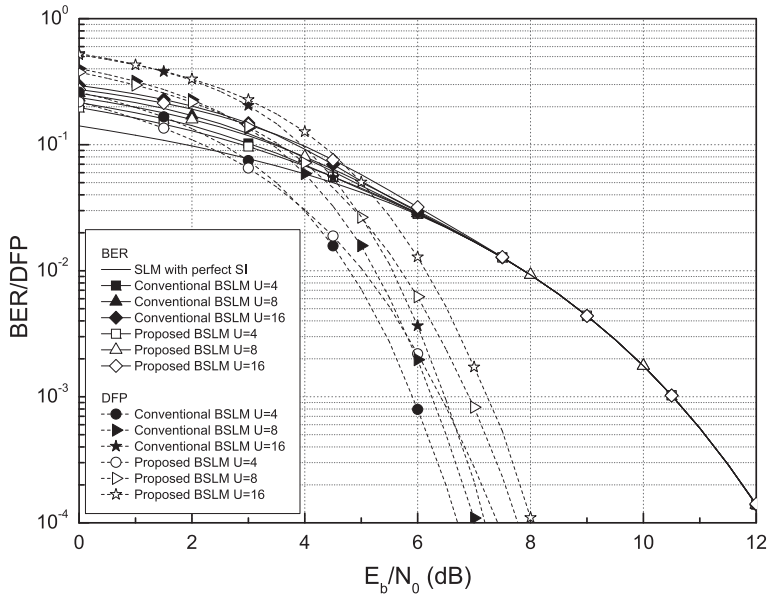

(b)

Figure 4.7: Comparison of DFP and BER of the proposed and the conventional BSLM schemes for $N = 64$ in the AWGN channel: (a) QPSK and (b) 16-QAM.

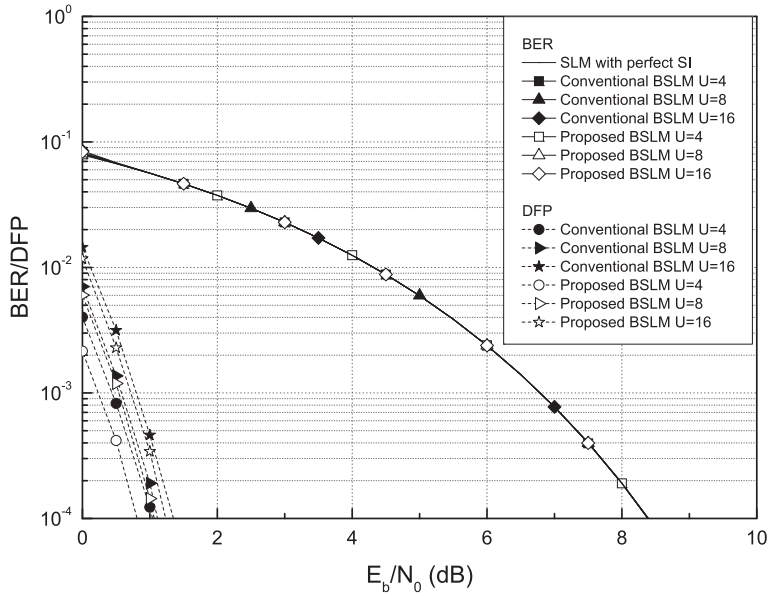

(a)

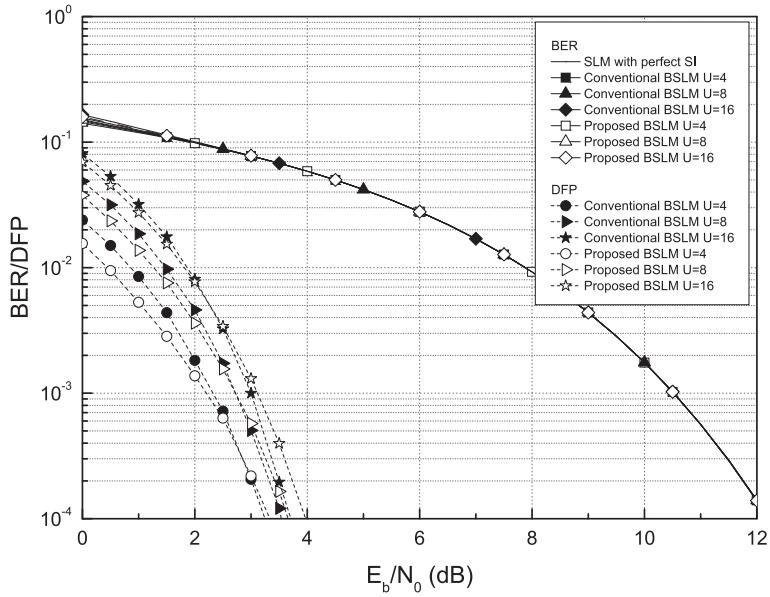

(b)

Figure 4.8: Comparison of DFP and BER of the proposed and the conventional BSLM schemes for $N = 256$ in the AWGN channel: (a) QPSK and (b) 16-QAM.

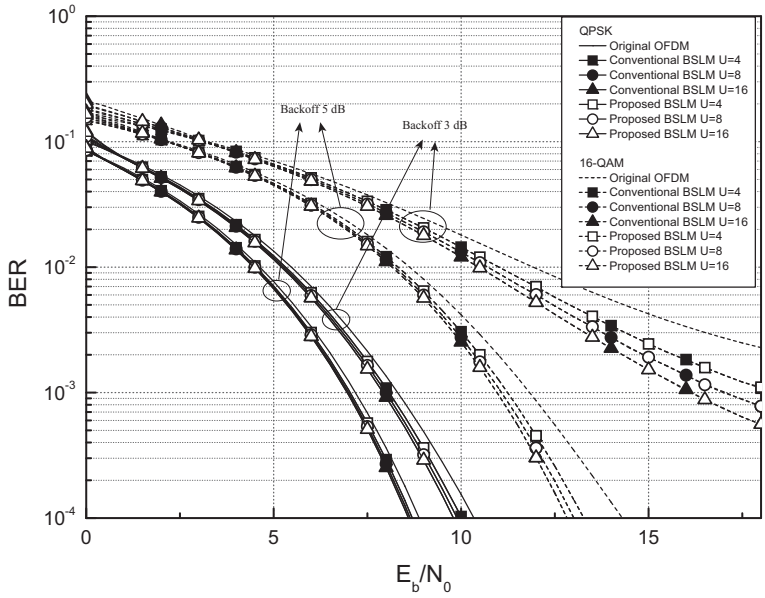

Figure 4.9: Comparison of BER of the proposed and the conventional BSLM schemes for $N = 256$ in the AWGN channel when a nonlinear HPA having backoff values with 3 and 5 dB is used.

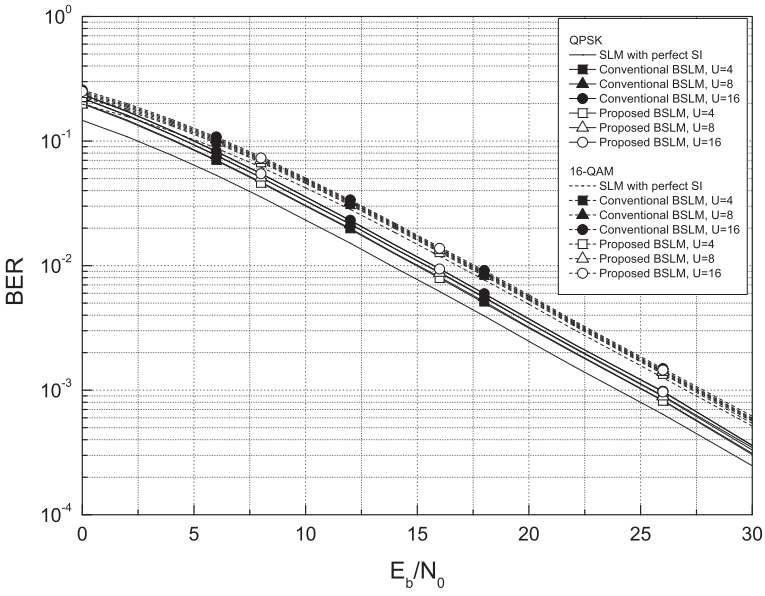

Figure 4.10: Comparison of BER of the proposed and the conventional BSLM schemes for $N = 256$ in the Rayleigh fading channel.

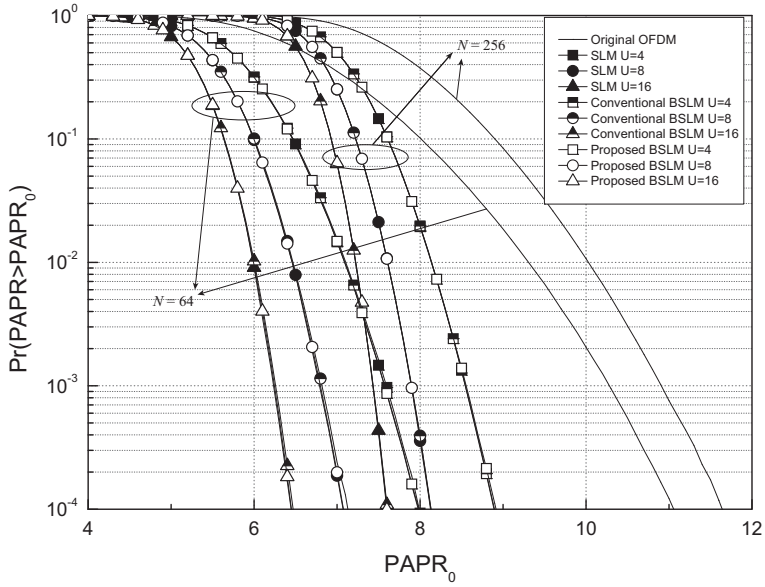

Figure 4.11: Comparison of PAPR reduction performance of the proposed and the conventional BSLM schemes for QPSK with $N = 64$ and $N = 256$.

Chapter 5. New Blind PTS Schemes

In order to recover the input symbol sequence successfully in the PTS scheme, the index of the selected rotating vector, called SI, should be transmitted to the receiver. Generally, several subcarriers for SI should be reserved in the PTS scheme. It is well known that the BER performance of the OFDM systems can be critically degraded as erroneously detecting the SI for the PTS scheme. Thus, strong error correcting code should be used for the SI and then the spectrum efficiency in the OFDM systems is degraded. To eliminate the transmission of SI, several BPTS schemes have been proposed [15], [16]. However, these proposed techniques insert some additional reference symbols to pilot symbols or have large detection complexity to recover the input symbol sequence at the receiver.

In this chapter, we propose two new BPTS schemes without SI. Similar to the method in Chapter 4, the proposed BPTS schemes embed the SI identifying a rotating vector into itself by using the phase offset on the elements of each rotating vector. To extract the SI from the rotating vector and recover the input data sequence, the ML detectors for the proposed BPTS schemes are derived. These detectors exploit the fact that the Euclidean distance between the given signal constellation and the signal constellation rotated by the phase offset exists. By using PEP analysis, it is explained how phase offsets for each BPTS scheme should be cho-

sen. Also, it is shown that for QPSK and 16-QAM, the BER performance of the proposed BPTS schemes is not degraded through the numerical analysis.

The rest of this chapter is organized as follows. In Section 5.1, the proposed BPTS scheme I (P-BPTS I) is proposed and the phase offsets and the subblock phase offset vectors to embed the SI into the rotating vectors are described. Also, the ML detector for the P-BPTS I scheme is explained. To lower the detection complexity of the proposed BPTS scheme, the proposed BPTS scheme II (P-BPTS II) to modify the P-BPTS I scheme is proposed in Section 5.2. Simulation results are given to show the performance of the proposed BPTS schemes in Section 5.3. Finally, conclusions are mentioned in Section 5.4.

5.1. Proposed Blind PTS Scheme I

5.1.1. Embedding Side Information into Rotating Vectors

In the conventional PTS scheme, an input signal sequence $\mathbf{X}$ is partitioned into V disjoint symbol subsequences $\mathbf{X}_v = [X_{v,0}\ X_{v,1}\ \cdots\ X_{v,N-1}]$, $0 \le v \le V-1$, which can be expressed as

$$\mathbf{X} = \sum_{v=0}^{V-1} \mathbf{X}_v. \tag{5.1}$$

For each symbol subsequence, $X_{v,k} = 0$, $0 \le k \le N-1$, except for N/V data symbols. The signal subsequence $\mathbf{x}_v = [x_{v,0}\ x_{v,1}\ \cdots\ x_{v,N-1}]$, called

a subblock, is generated by applying IFFT to each symbol subsequence $\mathbf{X}_v$. Each subblock $\mathbf{x}_v$ is multiplied by a rotating factor b_v^u. From the sum of the subblocks multiplied by b_v^u, the uth alternative signal sequence $\mathbf{x}^u = [x_0^u \; x_1^u \; \cdots \; x_{N-1}^u]$ can be obtained as

$$\mathbf{x}^u = \sum_{v=0}^{V-1} b_v^u \mathbf{x}_v \tag{5.2}$$

where $0 \leq u \leq U-1$ and $U = |\mathbb{B}|^{V-1}$. Let $\mathbf{b}^u = [b_0^u \; b_1^u \; \cdots \; b_{V-1}^u]$ be the uth rotating vector, where $\mathbf{b}^u \in \mathbb{B}^V$. In order to choose the alternative signal sequence with the minimum PAPR for transmission, the optimum rotating vector $\mathbf{b}^{\tilde{u}} = \left[b_0^{\tilde{u}} \; b_1^{\tilde{u}} \; \cdots \; b_{V-1}^{\tilde{u}}\right]$ can be obtained by using (3.5). Then, the selected alternative signal sequence $\mathbf{x}^{\tilde{u}}$ with the minimum PAPR is transmitted.

The goal of this section is to enable the PTS scheme to recover original data without any SI at the receiver. In order to eliminate the transmission of the SI, we consider the method to embed the SI into the rotating vectors by giving phase offsets similar to the proposed BSLM scheme in Chapter 4. First, we define a V-tuple phase offset vector as

$$\mathbf{S}^u = \left[S_0^u \; S_1^u \; \cdots \; S_{V-1}^u\right]$$

where $S_v^u \in \{0, 1, \cdots, Z\}$, $0 \leq v \leq V-1$, $0 \leq u \leq U-1$, Z is the number of the phase offsets. It is not difficult to check that if U rotating vectors are expressed from V-tuple phase offset vectors, Z must be selected such

that

$$(Z+1)^V \geq U = |\mathbb{B}|^{V-1}. \tag{5.3}$$

In order to embed the SI of the index u into the uth rotating vector, each rotating factor b_v^u, $0 \leq v \leq V-1$, $0 \leq u \leq U-1$, is multiplied by $e^{j\theta_{S_v^u}}$, where $\theta_0 = 0$ and $0 < \theta_{S_v^u} \leq \pi/2$ for $1 \leq S_v^u \leq Z$. Then, the uth modified rotating vector can be expressed as

$$\begin{aligned}\bar{\mathbf{b}}^u &= [\bar{b}_0^u \ \bar{b}_1^u \ \cdots \ \bar{b}_{V-1}^u] \\ &= \left[b_0^u e^{j\theta_{S_0^u}} \ b_2^u e^{j\theta_{S_1^u}} \ \cdots \ b_{V-1}^u e^{j\theta_{S_{V-1}^u}}\right]\end{aligned}$$

where $0 \leq u \leq U-1$. And the uth alternative signal sequence of the proposed BPTS scheme is expressed as

$$\mathbf{x}^u = \sum_{v=0}^{V-1} \bar{b}_v^u \mathbf{x}_v. \tag{5.4}$$

In the above BPTS scheme, called the P-BPTS I scheme, $\mathbf{x}^{\tilde{u}}$ with the minimum PAPR is selected for transmission.

Clearly, it is equivalent that for $\theta_{S_v^u} \neq 0$, $\bar{b}_v^u X_k$ is modulated by using the signal constellation $\mathcal{Q}_{\theta_{S_v^u}}$, which is obtained by rotating the signal constellation $\mathcal{Q}$ by $\theta_{S_v^u}$. When the selected signals are transmitted through noiseless channel without distortion, the received signal at the kth subcarrier is FFTed as $R_k = \bar{b}_v^{\tilde{u}} X_k$. Then, the detected symbol $\bar{b}_v^{u*} R_k$ in the receiver will not be on the signal constellation $\mathcal{Q}$ if $S_v^{\tilde{u}} \neq S_v^u$, where $\bar{b}_v^{u*}$ is the complex conjugate of $\bar{b}_v^u$. This observation allows the receiver to

obtain the SI and recover the input symbol sequence $\mathbf{X}$ from ML detector using the Euclidean distance between signal constellations, which will be explained in the next subsection.

5.1.2. ML Detection of the Proposed BPTS scheme

From the received signal with the modified rotating vector $\bar{\mathbf{b}}^{\tilde{u}}$, the receiver should find the index $\tilde{u}$ without any SI and recover the input symbol sequence $\mathbf{X}$. The received symbol R_k after performing FFT demodulation at the receiver can be expressed by

$$R_k = H_k \bar{b}_v^{\tilde{u}} X_k + N_k \tag{5.5}$$

where $0 \leq k \leq N-1$, H_k is the frequency response of the fading channel at the kth subcarrier, and N_k is an AWGN sample at the kth subcarrier. We assume that the channel is a quasi static Rayleigh fading channel and H_k is independent and perfectly known at the receiver. That is, the perfect CSI is assumed.

Now, we derive the ML detector for the proposed BPTS scheme using the Euclidean distance between signal constellations as follows. Let $\mathbf{R}_v = [R_{v,0}\ R_{v,1}\ \cdots\ R_{v,N-1}]$ denote the vth received symbol subsequence. The ML detector of the proposed BPTS scheme at the receiver is operated in two steps. First, the metric for each received symbol subsequence $\mathbf{R}_v$,

$0 \leq v \leq V-1$, is calculated as

$$D_{v,z} = \sum_{k \in \mathbb{C}_v} \min_{X'_k \in \mathcal{Q}} |R_{v,k} e^{-j\theta_z} - \hat{H}_k X'_k|^2 \tag{5.6}$$

where $z \in \{0, 1, \cdots, Z\}$, $|\cdot|$ denotes the absolute value of a complex number, $\hat{H}_k$ is the estimated channel response, and $\mathbb{C}_v = \{C_{v,0}, C_{v,1}, \cdots, C_{v,\frac{N}{V}-1}\}$ is the index set of N/V data symbols in the vth symbol subsequence $\mathbf{X}_v$. The ML detecting process in (5.6) is operated as follows. Let $\hat{X}^z_{v,k}$ be the constellation point in $\mathcal{Q}$ which minimizes the Euclidean distance between $R_{v,k}e^{-j\theta_z}$ and $\hat{H}_k X'_k$. For the given z, the detected symbol $\hat{X}^z_{v,k}$ with the minimum metric for each subcarrier in the vth symbol subsequence is obtained and its metric $|R_{v,k}e^{-j\theta_z} - \hat{H}_n \hat{X}^z_{v,k}|^2$ is added to $D_{v,z}$. Then, for each vth symbol subsequence, we obtain $D_{v,0}, D_{v,1}, \cdots, D_{v,Z}$, and also the detected symbol subsequence $\hat{\mathbf{X}}^0_v, \hat{\mathbf{X}}^1_v, \cdots, \hat{\mathbf{X}}^Z_v$, where $\hat{\mathbf{X}}^z_v = [\hat{X}^z_{v,0}\ \hat{X}^z_{v,1}\ \cdots\ \hat{X}^z_{v,N-1}]$. It is easy to check that $\hat{\mathbf{X}}^z_v$ consists of N/V detected symbols and $N(V-1)/V$ zeros. This process is repeated for all v, $0 \leq v \leq V-1$.

By using $D_{v,z}$'s in (5.6), the index $\hat{u}$ can be obtained by the decision metric $D_{\hat{u}}$ with the minimum value among U metric sum values D_u corresponding to $\mathbf{S}^u$ as

$$\hat{u} = \arg \min_{0 \leq u \leq U-1} D_u = \arg \min_{0 \leq u \leq U-1} \sum_{v=0}^{V-1} D_{v,S^u_v}. \tag{5.7}$$

Although the detected symbol subsequences $\hat{\mathbf{X}}^{S^u_v}_v$ is obtained by eliminating the phase offset $\theta_{S^u_v}$ from each received symbol subsequence $\mathbf{R}_v$ by the

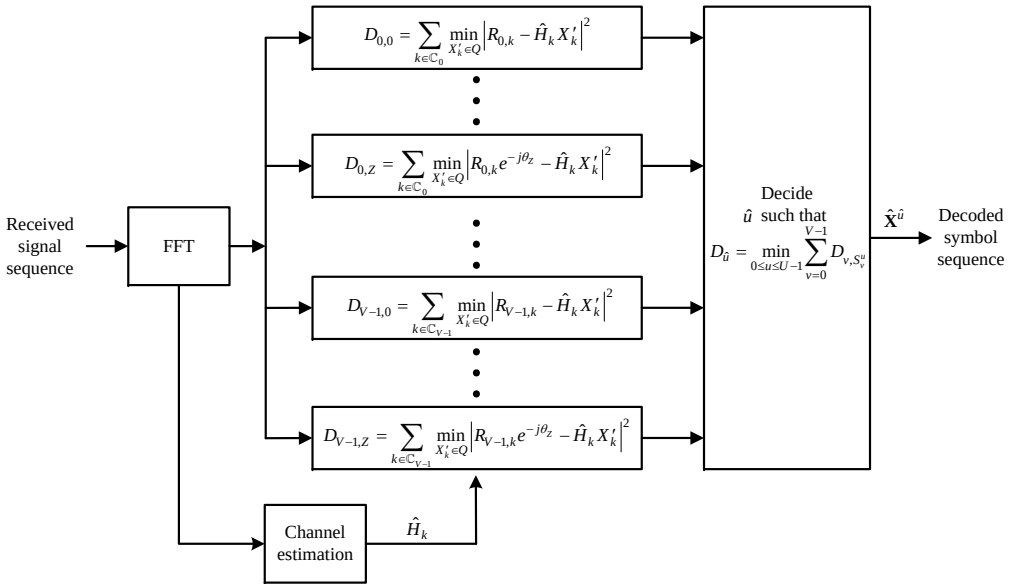

Figure 5.1: A block diagram of the ML detector for the P-BPTS I scheme.

ML detector, the rotating factors $b_v^{\tilde{u}}$ are included in $\hat{\mathbf{X}}_v^{S_v^u}$. Therefore, the detected input symbol sequence at the receiver is finally obtained as

$$\hat{\mathbf{X}}^{\hat{u}} = \sum_{v=0}^{V-1} b_v^{\hat{u}*} \hat{\mathbf{X}}_v^{S_v^{\hat{u}}},$$

which is summation of V detected symbol subsequences derotated by $b_v^{\hat{u}*}$, $0 \le v \le V-1$. Fig. 5.1 shows a block diagram of the proposed ML detector.

Consequently, the overall detection complexity to find the index $\hat{u}$ and the detected symbol sequence $\hat{\mathbf{X}}^{\hat{u}}$ in (5.6) and (5.7) is $(Z+1)qN$ $|\cdot|^2$ operations if the real additions are ignored because the complexity of $|\cdot|^2$ operation is much larger than that of real addition.

5.1.3. Design Criteria of V-Tuple Phase Offset Vectors and Phase Offsets

Now we have to design the optimal V-tuple phase offset vectors and phase offsets.

In this subsection, design criteria of V-tuple phase offset vectors and phase offsets will be proposed by using the PEP of the ML detector in (5.6) and (5.7). It is well known that to analyze the BER performance of communication systems with coding schemes such as trellis codes and space-time codes, PEP approach is widely used [37]. For convenience of PEP analysis, we assume that the subblock partitioning method of the P-BPTS I scheme is used as adjacent subblock partitioning. Also, we assume that the channel is modeled as the Rayleigh fading channel, that is, the coefficients H_k are independent samples of complex Gaussian random variables with zero mean and variance 0.5 per dimension. We consider that each element of the signal constellation is contracted by a scale factor $\sqrt{E_s}$ so that the average energy of the constellation elements is 1, where E_s is the average energy of the signal constellation. Therefore, our PEP analysis for the proposed ML detector can be independent from the average energy of the signal constellations.

The PEP of the proposed ML detector is the probability to determine $\hat{\mathbf{X}}\otimes\mathbf{B}^{\hat{u}}$ when $\mathbf{X}\otimes\mathbf{B}^{\tilde{u}}$ is transmitted, where $\mathbf{B}^u = \left[\bar{b}_0^u \cdots \bar{b}_0^u \bar{b}_1^u \cdots \bar{b}_1^u \cdots \bar{b}_{V-1}^u \cdots \bar{b}_{V-1}^u\right]$, $0 \le u \le U-1$, is an N-tuple vector of rotating factors and $\mathbf{X} \otimes \mathbf{B}^u$ denotes the componentwise multiplication of vectors $\mathbf{X}$ and $\mathbf{B}^u$. Assuming

the perfect CSI at the receiver, the probability of transmitting $\mathbf{X}\otimes\mathbf{B}^{\tilde{u}}$ and determining $\hat{\mathbf{X}}\otimes\mathbf{B}^{\hat{u}}$ at the proposed ML detector is well approximated as [37]

$$\Pr\left(\mathbf{X}\otimes\mathbf{B}^{\tilde{u}}\rightarrow\hat{\mathbf{X}}\otimes\mathbf{B}^{\hat{u}}|H_k,k=0,1,\cdots,N-1\right)\leq \exp\left(-\frac{d^2(\mathbf{X}\otimes\mathbf{B}^{\tilde{u}},\hat{\mathbf{X}}\otimes\mathbf{B}^{\hat{u}})E_s}{4N_0}\right) \tag{5.8}$$

where $N_0/2$ is the noise variance per dimension and

$$d^2(\mathbf{X}\otimes\mathbf{B}^{\tilde{u}},\hat{\mathbf{X}}\otimes\mathbf{B}^{\hat{u}})=\sum_{v=0}^{V-1}\sum_{k=\frac{Nv}{V}}^{\frac{N(v+1)}{V}-1}\left|H_k\left(X_k b_v^{\tilde{u}}e^{j\theta_{S_v^{\tilde{u}}}}-\hat{X}_k b_k^{\hat{u}}e^{j\theta_{S_v^{\hat{u}}}}\right)\right|^2.$$

Let $A_k=X_k b_v^{\tilde{u}}e^{j\theta_{S_v^{\tilde{u}}}}-\hat{X}_k b_k^{\hat{u}}e^{j\theta_{S_v^{\hat{u}}}}$, $0\leq n\leq N-1$, $0\leq v\leq V-1$. Since $A_k\neq 0$ for $S_v^{\tilde{u}}\neq S_v^{\hat{u}}$ and $A_k=0$ for $S_v^{\tilde{u}}=S_v^{\hat{u}}$, the PEP in (5.8) is rewritten as

$$\Pr\left(\mathbf{X}\otimes\mathbf{B}^{\tilde{u}}\rightarrow\hat{\mathbf{X}}\otimes\mathbf{B}^{\hat{u}}|H_k,k=0,1,\cdots,N-1\right)\leq \prod_{v\in\mathbb{V}^{\tilde{u}}}\prod_{k=\frac{N(v-1)}{V}}^{\frac{Nv}{V}-1}\exp\left(\frac{-|H_kA_k|^2E_s}{4N_0}\right) \tag{5.9}$$

where $\mathbb{V}^{\tilde{u}}$ is a set of v such that $S_v^{\tilde{u}}\neq S_v^{\hat{u}}$. As H_k is an independent complex Gaussian random variables with variance 0.5 per dimension and zero mean, $|H_k|$'s are independent Rayleigh distributed with PDF

$$\Pr(|H_k|)=2|H_k|\exp\left(-|H_k|^2\right)\quad\text{for }|H_k|\geq 0.$$

Therefore, the PEP in (5.9) can be averaged with respect to independent Rayleigh distributions of $|H_k|$ as

$$\Pr\left(\mathbf{X}\otimes\mathbf{B}^{\tilde{u}}\rightarrow\hat{\mathbf{X}}\otimes\mathbf{B}^{\hat{u}}\right)\leq\prod_{v\in\mathbb{V}^{\tilde{u}}}\left(\frac{1}{\prod_{k=\frac{N(l-1)}{L}}^{\frac{Nv}{L}-1}(1+|A_k|^2E_s/4N_0)}\right)$$
$$\cong\prod_{v\in\mathbb{V}^{\tilde{u}}}\left(\frac{1}{\prod_{k=\frac{N(l-1)}{V}}^{\frac{Nv}{V}-1}(|A_k|^2E_s/4N_0)}\right). \quad (5.10)$$

From (5.10), the upper bound of the PEP for the proposed ML detector is obtained as

$$\Pr\left(\mathbf{X}\otimes\mathbf{B}^{\tilde{u}}\rightarrow\hat{\mathbf{X}}\otimes\mathbf{B}^{\hat{u}}\right)\leq\prod_{v\in\mathbb{V}^{\tilde{u}}}\left(\prod_{k=\frac{N(v-1)}{V}}^{\frac{Nv}{V}-1}|A_k|^2\right)^{-1}\left(\frac{E_s}{4N_0}\right)^{-|\mathbb{V}^{\tilde{u}}|\frac{N}{V}}. \quad (5.11)$$

From the above analysis, it is easy to check that in order to decrease error in (5.11), $|\mathbb{V}^{\tilde{u}}|N/L$ and $|A_k|^2$ should be maximized, respectively. Thus, we propose the following design criteria for V-tuple phase offset vectors $\mathbf{S}^u$ and phase offsets $\theta_{S_v^u}$.

- The minimum Hamming distance between $\mathbf{S}^i$ and $\mathbf{S}^j$ for $i\neq j$ should be maximized for the given $U=|\mathbb{B}|^{V-1}$.
- In order to obtain large $|A_k|^2$ in average sense, the average Euclidean distance between signal constellations $Q_{\theta_{S_v^i}}$ and $Q_{\theta_{S_v^j}}$ for $i\neq j$ should be maximized.

If the number of phase offsets, i.e., Z, is large, the set of V-tuple phase offset vectors to satisfy the first criterion can easily be constructed. How-

ever, as Z increases, the average Euclidean distance between signal constellations for the second criterion is reduced and detection complexity of the proposed ML detector also increases. That is, it is difficult to find V-tuple phase offset vectors and phase offsets to satisfy two design criteria simultaneously.

5.1.4. Design of V-Tuple Phase Offset Vectors and Phase Offsets

To achieve the first design criteria, a set of V-tuple phase offset vectors to use large Z is considered. By increasing Z, the average Euclidean distance between signal constellations can be considerably reduced [38] and the detection complexity of the proposed ML detector increases. In fact, we can consider that the second criterion is more important than the first criterion in terms of signal constellations and detection complexity. Thus, we have to take a tradeoff for Z. That is, the P-BPTS I scheme adopts the minimum $Z = \lceil |\mathbb{B}|^{\frac{V-1}{V}} \rceil - 1$ such that (5.3), where $\lceil \cdot \rceil$ is the ceiling function. For the P-BPTS I scheme with $Z = \lceil |\mathbb{B}|^{\frac{V-1}{V}} \rceil - 1$, the phase offsets such that $\theta_{S_v^u} \in \{\frac{i\pi}{2(Z+1)} | i = 0, 1, \cdots, Z\}$ are used. In order to construct the set of V-tuple phase offset vectors for the P-BPTS I scheme, U phase offset vectors are randomly chosen among $(Z+1)^V$ vectors with length V and $0 \leq S_v^u \leq Z$.

By using the minimum Z to satisfy (5.3) in the P-BPTS I scheme, we can check that $Z = 1$ for $\mathbb{B} = \{\pm 1\}$. That is, in case of binary rotating vectors, U vectors among 2^V binary vectors are selected as V-tuple phase off-

	b_0^u	b_1^u	b_2^u
$u=0$	1	1	1
$u=1$	1	1	-1
$u=2$	1	1	j
$u=3$	1	1	$-j$
$u=4$	1	-1	1
$u=5$	1	-1	-1
$u=6$	1	-1	j
$u=7$	1	-1	$-j$
$u=8$	1	j	1
$u=9$	1	j	-1
$u=10$	1	j	j
$u=11$	1	j	$-j$
$u=12$	1	$-j$	1
$u=13$	1	$-j$	-1
$u=14$	1	$-j$	j
$u=15$	1	$-j$	$-j$

S_0^u	S_1^u	S_2^u
0	0	0
0	0	1
0	1	0
1	0	1
2	1	0
1	1	1
0	1	2
1	2	2
0	2	0
2	1	1
1	0	0
1	2	0
0	2	1
1	1	0
2	2	0
2	2	2

$\hat{b}_0^u$	$\hat{b}_1^u$	$\hat{b}_2^u$
1	1	1
1	1	$-1\times e^{j\frac{\pi}{6}}$
1	$1\times e^{j\frac{\pi}{6}}$	j
$1\times e^{j\frac{\pi}{6}}$	1	$-j\times e^{j\frac{\pi}{6}}$
$1\times e^{j\frac{\pi}{3}}$	$-1\times e^{j\frac{\pi}{6}}$	1
$1\times e^{j\frac{\pi}{6}}$	$-1\times e^{j\frac{\pi}{6}}$	$-1\times e^{j\frac{\pi}{6}}$
1	$-1\times e^{j\frac{\pi}{6}}$	$j\times e^{j\frac{\pi}{3}}$
$1\times e^{j\frac{\pi}{6}}$	$-1\times e^{j\frac{\pi}{3}}$	$-j\times e^{j\frac{\pi}{3}}$
1	$j\times e^{j\frac{\pi}{3}}$	1
$1\times e^{j\frac{\pi}{3}}$	$j\times e^{j\frac{\pi}{6}}$	$-1\times e^{j\frac{\pi}{6}}$
$1\times e^{j\frac{\pi}{6}}$	j	j
$1\times e^{j\frac{\pi}{6}}$	$j\times e^{j\frac{\pi}{3}}$	$-j$
1	$-j\times e^{j\frac{\pi}{3}}$	$1\times e^{j\frac{\pi}{6}}$
$1\times e^{j\frac{\pi}{6}}$	$-j\times e^{j\frac{\pi}{6}}$	-1
$1\times e^{j\frac{\pi}{3}}$	$-j\times e^{j\frac{\pi}{3}}$	j
$1\times e^{j\frac{\pi}{3}}$	$-j\times e^{j\frac{\pi}{3}}$	$-j\times e^{j\frac{\pi}{3}}$

Figure 5.2: 16 rotating vectors, V-tuple phase offset vectors, and modified rotating vectors for the P-BPTS I scheme with $V = 3$, $\mathbb{B} = \{\pm 1, \pm j\}$, and $Z = 2$.

set vectors and $\theta_{S_v^u} \in \{0, \pi/4\}$. On the other hands, when $\mathbb{B} = \{\pm 1, \pm j\}$, it is not difficult to check that $Z = 2$ for $V < 5$ and $Z = 3$ for $V \geq 5$ to satisfy (5.3).

For example, consider the P-BPTS I scheme with $V = 3$, $\mathbb{B} = \{\pm 1, \pm j\}$, and $Z = 2$, which uses 16 V-tuple phase offset vectors randomly chosen among all 27 ternary vectors with length 3 and phase offsets $\theta_{S_v^u} \in$

$\{0, \pi/6, \pi/3\}$. Fig. 5.2 shows 16 rotating vectors, V-tuple phase offset vectors, and modified rotating vectors for the P-BPTS I scheme with $V = 3$, $\mathbb{B} = \{\pm 1, \pm j\}$, and $Z = 2$, respectively.

For the P-BPTS I scheme, the total detection complexity to find the index $\hat{u}$ and the detected symbol sequence $\hat{\mathbf{X}}^{\hat{u}}$ in (5.6) and (5.7) is $\lceil |\mathbb{B}|^{\frac{V-1}{V}} \rceil qN$ $|\cdot|^2$ operations if the real additions are ignored.

5.2. Proposed BPTS Scheme II

In Chapter 4, to minimize the detection complexity of the proposed BSLM scheme, the number of the phase offsets should be only 1, that is, $\theta = \pi/4$. Similar to the proposed BSLM scheme, since it is possible to use $Z = 1$ for $\mathbb{B} = \{\pm 1\}$, the minimum number of the phase offsets for the P-BPTS I scheme can be $Z = 1$, which leads to low detection complexity at the receiver. However, in the case of $\mathbb{B} = \{\pm 1, \pm j\}$, the number of the phase offsets for the P-BPTS I scheme should be 2 or 3, which increases the detection complexity of the P-BPTS I scheme. Therefore, to achieve low detection complexity for $\mathbb{B} = \{\pm 1, \pm j\}$, we propose another new BPTS scheme with $Z = 1$, called P-BPTS II scheme.

For the P-BPTS II scheme with $\mathbb{B} = \{\pm 1, \pm j\}$, we consider that the phase offset θ_1 is $\pi/4$, that is, $Z = 1$. It is known in [38] that when $Z = 1$, the Euclidean distance between two signal constellations $\mathcal{Q}$ and $\mathcal{Q}_{\theta_1}$ is maximized. However, if $V \geq 3$, the V-tuple phase offset vectors with $Z = 1$ and the phase offset $\theta_{S_v^u} \in \{0, \pi/4\}$ cannot represent all of U

rotating vectors with $\mathbb{B} = \{\pm 1, \pm j\}$ because (5.3) cannot be satisfied.

The approach to embed SI in Subsection 5.1.1 cannot be directly applied to the P-BPTS II scheme with $Z = 1$ and $|\mathbb{B}| = 4$. Therefore, we propose a new method to generate alternative signal sequences for the P-BPTS II scheme as follows. By using the linear property of discrete Fourier transform (DFT), the vth subblock is divided into even subblock $\mathbf{x}_v^e = [x_{v,0}^e \; x_{v,1}^e \; \cdots \; x_{v,N-1}^e]$ and odd subblock $\mathbf{x}_v^o = [x_{v,0}^o \; x_{v,1}^o \; \cdots \; x_{v,N-1}^o]$, which correspond to IFFTs of even symbols and odd symbols in the frequency domain, respectively, as

$$\begin{aligned} x_{v,n}^e &= x_{v,n+\frac{N}{2}}^e = \frac{1}{2}\left(x_{v,n} + x_{v,n+\frac{N}{2}}\right) \\ x_{v,n}^o &= -x_{v,n+\frac{N}{2}}^o = \frac{1}{2}\left(x_{v,n} - x_{v,n+\frac{N}{2}}\right) \end{aligned} \tag{5.12}$$

where $0 \le n < N/2$ and $0 \le v \le V-1$. The uth alternative signal sequence of the P-BPTS II scheme can be generated as

$$\mathbf{x}^u = \sum_{v=0}^{V-1} b_v^u \left(e^{j\frac{\pi}{4}S_{v,e}^u}\mathbf{x}_v^e + e^{j\frac{\pi}{4}S_{v,o}^u}\mathbf{x}_v^o\right) \tag{5.13}$$

where

$$(S_{v,e}^u, S_{v,o}^u) = \begin{cases} (0,0), & S_v^u = 0 \\ (1,1), & S_v^u = 1 \\ (0,1), & S_v^u = 2 \\ (1,0), & S_v^u = 3. \end{cases}$$

Since the alternative signal sequences for the P-BPTS II scheme are gen-

erated differently from the P-BPTS I scheme, the metric in (5.6) is also modified as

$$D_{v,z} = \begin{cases} \sum_{k\in\mathbb{C}_v} \min_{X'_k\in\mathcal{Q}} |R_k - \hat{H}_k X'_k|^2, & z = 0 \\ \sum_{k\in\mathbb{C}_v} \min_{X'_k\in\mathcal{Q}} |R_k e^{-j\frac{\pi}{4}} - \hat{H}_k X'_k|^2, & z = 1 \\ \sum_{k\in\mathbb{C}_v^e} \min_{X'_k\in\mathcal{Q}} |R_k - \hat{H}_k X'_k|^2 + \sum_{k\in\mathbb{C}_v^o} \min_{X'_k\in\mathcal{Q}} |R_k e^{-j\frac{\pi}{4}} - \hat{H}_k X'_k|^2, & z = 2 \\ \sum_{k\in\mathbb{C}_v^e} \min_{X'_k\in\mathcal{Q}} |R_k e^{-j\frac{\pi}{4}} - \hat{H}_k X'_k|^2 + \sum_{k\in\mathbb{C}_v^o} \min_{X'_k\in\mathcal{Q}} |R_k - \hat{H}_k X'_k|^2, & z = 3 \end{cases} \tag{5.14}$$

where $\mathbb{C}_v^e$ and $\mathbb{C}_v^o$ denote the subsets of even indices and odd indices of $\mathbb{C}_v$, respectively. Although $D_{v,z}$'s are obtained from the modified metrics using (5.14), the process to extract the index $\hat{u}$ and to determine the input symbol sequence in the P-BPTS II scheme is the same as that of the P-BPTS I scheme. As a result, the detection complexity of the P-BPTS II scheme is only $2qN$ $|\cdot|^2$ operations similar to the proposed BSLM in Chapter 4.

5.3. Simulation Results

In this section, we show several simulation results to evaluate the performance in terms of PAPR reduction and BER of the ML detector in the proposed two BPTS schemes without SI. The simulation results are based on the OFDM systems with $N = 256$, which are modulated by QPSK and 16-QAM.

In Fig. 5.3, the PAPR reduction performance of the proposed BPTS

schemes and the conventional PTS scheme for QPSK and 16-QAM is shown. The PAPR reduction performance of the P-BPTS I scheme is slightly worse than that of the P-BPTS II scheme. It is because the average Euclidean distance between alternative signal sequences in the P-BPTS I scheme is reduced by using the large number of phase offsets, Z, compared to those of P-BPTS II scheme. Especially, the PAPR reduction performance in the P-BPTS I scheme is more degraded than that of the P-BPTS II scheme for QPSK because the correlation between alternative signal sequences in QPSK increases due to the less Euclidean distance as the number of phase offsets increases. In contrast, for 16-QAM, the performance degradation between two proposed schemes is negligible, that is, within 0.1 dB.

Fig. 5.4 compares the BERs of the two proposed BPTS schemes with $N = 256$ modulated by QPSK and 16-QAM in the AWGN channel. Since the practical OFDM systems usually require the BER better than 10^{-3}, the BER degradation from the detection failure in the practical SNR region can be negligible. The BER performance of the P-BPTS I scheme is almost the same as that of the P-BPTS II scheme.

Fig. 5.5 shows the BER performance of the proposed BSLM scheme with $N = 256$ modulated by QPSK and 16-QAM in the AWGN channel for a nonlinear HPA with backoff values of 3 and 5 dB. The BER performance of the proposed BPTS schemes is better than those of QPSK and 16-QAM in the AWGN channel with a nonlinear HPA.

Fig. 5.6 shows the BER performance of the proposed BPTS schemes

with $N = 256$, QPSK, and 16-QAM in the Rayleigh fading channel. The conventional PTS scheme with PSI performs slightly better than the two proposed BPTS schemes in the Rayleigh fading channel.

5.4. Conclusion

In this chapter, two BPTS schemes without SI are proposed for PAPR reduction of OFDM signals. The proposed BPTS schemes embed the SI identifying a rotating vector into itself by using the phase offset on the elements of each rotating vector. To extract the SI from the rotating vector and to recover the data sequence, the ML detectors for the proposed BPTS schemes are derived. The simulation results show that for QPSK and 16-QAM, the BER and PAPR reduction performance of the proposed BPTS schemes without SI is not degraded.

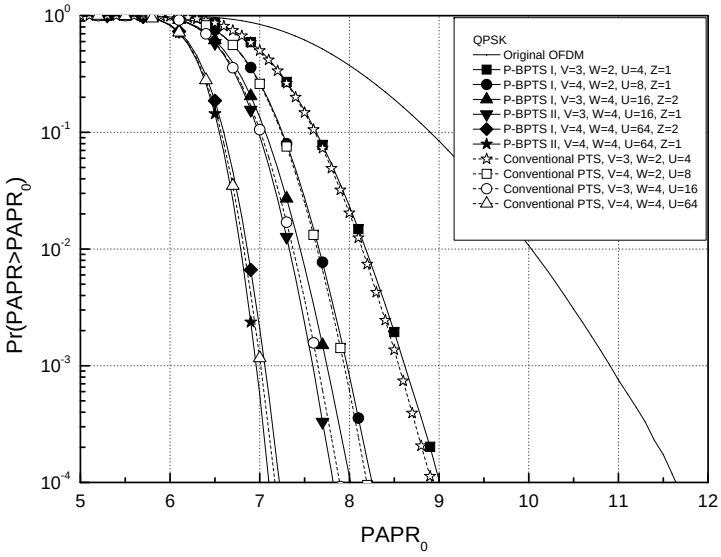

(a)

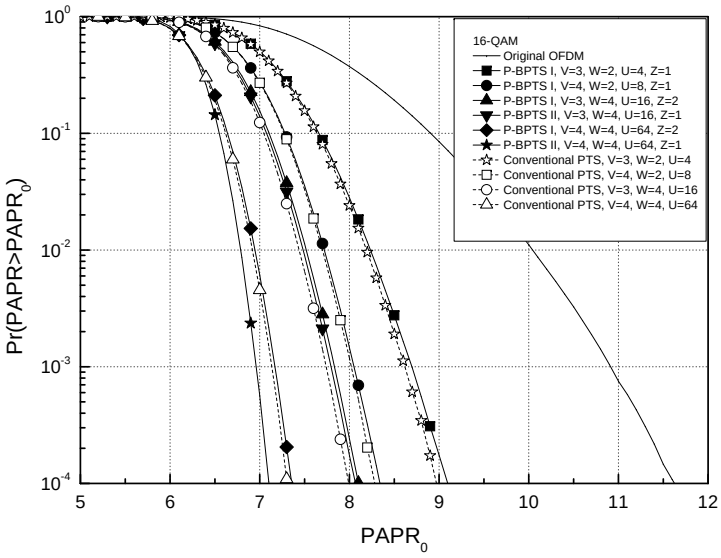

(b)

Figure 5.3: Comparison of PAPR reduction performance of the proposed BPTS schemes and the conventional PTS scheme with $N = 256$: (a) QPSK and (b) 16-QAM.

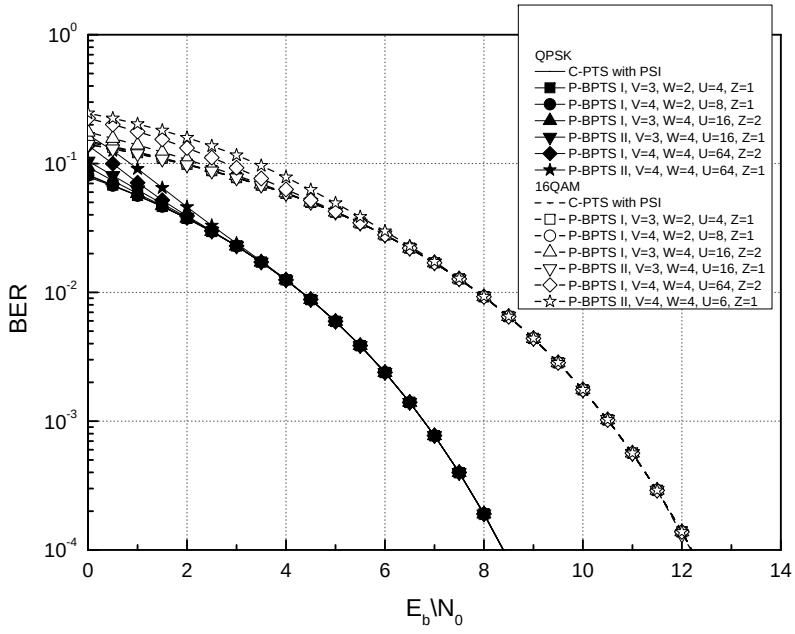

Figure 5.4: Comparison of BER of the proposed BPTS scheme and the conventional PTS scheme with perfect SI for $N = 256$ in the AWGN channel.

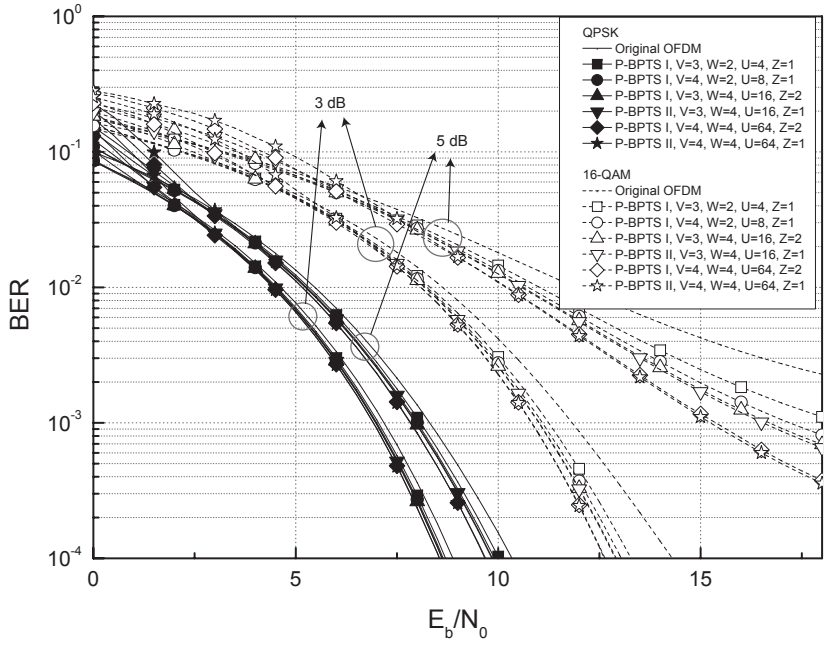

Figure 5.5: Comparison of BER of the proposed BPTS scheme and the conventional PTS scheme with perfect SI for $N = 256$ in the AWGN channel when a nonlinear HPA having backoff values with 3 and 5 dB is used.

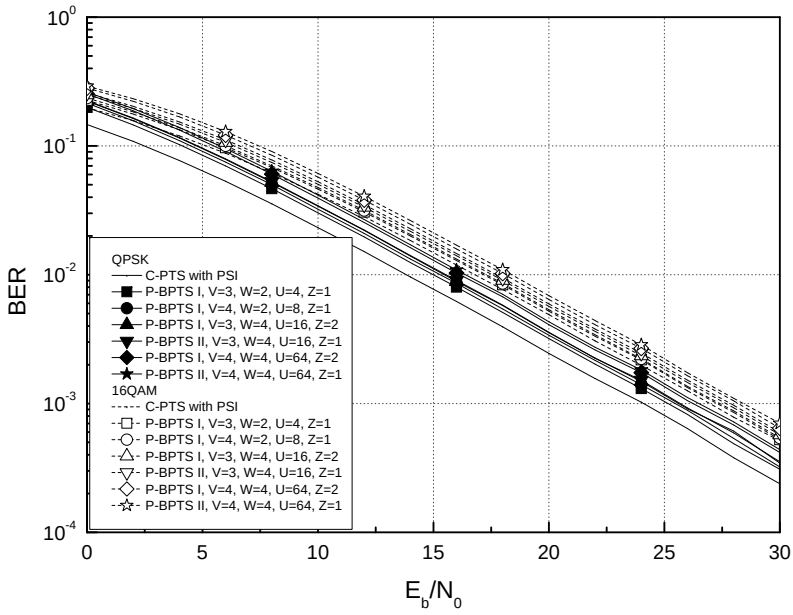

Figure 5.6: Comparison of BER of the proposed BPTS scheme and the conventional PTS scheme with perfect SI for $N = 256$ in the Rayleigh fading channel.

Chapter 6. Subblock Partitioning Scheme with Low Complexity

In the OFDMA system and PTS scheme, OFDM signals are partitioned into V signal subsequences, which requires large computational complexity due to V IFFT operations. In order to reduce the computational complexity in the subblock partitioning scheme of OFDM systems, we propose a new subblock partitioning scheme with low complexity using the subblock partition matrix. Using the convolution property of the IFFT [39], [40], the subblock partition matrix is derived. The signal subsequences are obtained by the circular convolution of the OFDM signal sequence and the subblock partition matrix. As IFFT operations to generate V signal subsequences are replaced by the circular convolution, only one IFFT operation is performed without additional IFFT. The interleaved subblock partitioning scheme is suitable for the use of the subblock partition matrix because most of the elements in the corresponding subblock partition matrix are zero.

The rest of this chapter is organized as follows. In Section 6.1, a subblock partitioning scheme is briefly reviewed. In Section Section 6.2, subblock partition matrices are proposed for new subblock partitioning scheme. In Section 6.3, low-complexity subblock partitioning scheme using sub-

block partition matrix is proposed. Computational complexity of the proposed subblock partitioning scheme are analyzed in Section 6.4. Finally, conclusions are given in Section 6.5.

6.1. Subblock Partitioning of OFDM Signal

Consider that an input symbol sequence $\mathbf{X}$ is partitioned into V disjoint symbol subsequences $\mathbf{X}_v = [X_{v,0}\ X_{v,1}\cdots X_{v,N-1}]^T,\ v = 0, 1, \cdots, V-1$, as

$$\mathbf{X} = \sum_{v=0}^{V-1} \mathbf{X}_v. \tag{6.1}$$

Let $\mathbf{P}_v = [P_{v,0}\ P_{v,1}\cdots P_{v,N-1}]$ be a subblock partition vector, where $P_k \in \{0, 1\}$, $0 \le k \le N-1$. Then, the vth subsequence $\mathbf{X}_v$ can be written as

$$\begin{aligned} \mathbf{X}_v &= [P_{v,0}X_0\ P_{v,1}X_1\ \cdots\ P_{v,N-1}X_{N-1}]^T \\ &= \mathbf{M}_v\mathbf{X} \end{aligned} \tag{6.2}$$

where

$$\mathbf{M}_v = \begin{bmatrix} P_{v,0} & & & 0 \\ & P_{v,1} & & \\ & & \ddots & \\ 0 & & & P_{v,N-1} \end{bmatrix} \tag{6.3}$$

is the diagonal matrix form corresponding to the subblock partition vector. Each data symbol in the input symbol sequence $\mathbf{X}$ should belong to only one symbol subsequence $\mathbf{X}_v$. It is clear that $X_{v,k} = 0$, $0 \le k \le N-1$,

except for subcarriers to allocate the data symbol in the vth symbol subsequence. After IFFTing $\mathbf{X}_v$, the vth signal subsequence, called a subblock, is obtained as

$$\mathbf{x}_v = \text{IFFT}(\mathbf{X}_v) = [x_{v,0}\ x_{v,1}\ \cdots\ x_{v,N-1}]^T \tag{6.4}$$

where $v = 0, 1, \cdots, V-1$. From the linear property of the IFFT, V subblocks are summed to result in OFDM signal sequence $\mathbf{x} = [x_0\ x_1\ \cdots\ x_{N-1}]^T$ as

$$\mathbf{x} = \sum_{v=0}^{V-1} \mathbf{x}_v. \tag{6.5}$$

There have been several subblock partitioning schemes such as adjacent, interleaving, and random subblock partitioning [41]. Fig. 6.1 is an example of the adjacent, interleaved, and random subblock partitioning schemes with $N = 16$ and $V = 4$. To generate V subblocks in the random and adjacent subblock partitioning schemes, V IFFT operations are required. The OFDM systems are burdened with additional IFFT operations. Since the reduced computational complexity is possible in the interleaved subblock partitioning scheme compared with other schemes, it has been adopted in several OFDM systems. Therefore, for the interleaved subblock partitioning scheme, subblock partition matrices, which replaces the IFFT to generate V subblocks by the circular convolution in the OFDM systems, is proposed in the next section.

6.2. Subblock Partition Matrix for Interleaved Subblock Partitioning

In this section, we propose how to construct subblock partition matrices to replace the IFFT for the generation of subblocks in the subblock partitioning scheme. Similar to the conversion matrix for the SLM scheme in [30], the proposed subblock partitioning scheme uses the OFDM signal sequence $\mathbf{x}$ after IFFT in order to generate the vth subblock $\mathbf{x}_v$, $0 \leq v \leq V-1$. The vth subblock $\mathbf{x}_v$ can be rewritten as

$$\mathbf{x}_v = \text{IFFT}(\mathbf{X}_v) = \mathbf{Q}\mathbf{M}_v\mathbf{X} \tag{6.6}$$

where

$$\mathbf{Q} = \frac{1}{N}\begin{bmatrix} 1 & 1 & 1 & \cdots & 1 \\ 1 & W_N^{-1} & W_N^{-2} & \cdots & W_N^{-(N-1)} \\ 1 & W_N^{-2} & W_N^{-4} & \cdots & W_N^{-2(N-1)} \\ \vdots & \vdots & \vdots & \ddots & \vdots \\ 1 & W_N^{-(N-1)} & W_N^{-2(N-1)} & \cdots & W_N^{-(N-1)\times(N-1)} \end{bmatrix} \tag{6.7}$$

is the IFFT matrix with $W_N = e^{-j\frac{2\pi}{N}}$. Since $\mathbf{x} = \text{IFFT}(\mathbf{X}) = \mathbf{Q}\mathbf{X}$, the input symbol sequence is expressed as

$$\mathbf{X} = \mathbf{Q}^{-1}\mathbf{x} \tag{6.8}$$

where $\mathbf{Q}^{-1}$ denotes the FFT matrix. From (6.6) and (6.8), the vth subblock $\mathbf{x}_v$ can be obtained as

$$\mathbf{x}_v = \mathbf{Q}\mathbf{M}_v\mathbf{Q}^{-1}\mathbf{x}. \tag{6.9}$$

Therefore, in order to directly derive $\mathbf{x}_v$ from $\mathbf{x}$, the subblock partition matrix should be obtained as

$$\mathbf{T}_v = \mathbf{Q}\mathbf{M}_v\mathbf{Q}^{-1}. \tag{6.10}$$

From the convolution property of the IFFT, the subblock partition matrix $\mathbf{T}_v$ can be expressed by using the subblock partition vector $\mathbf{P}_v$. That is, the vth subblock $\mathbf{x}_v$ can be obtained by a circular convolution of the OFDM signal sequence $\mathbf{x}$ and the IFFT of the subblock partition vector $\mathbf{P}_v$ as

$$\mathbf{x}_v = \mathrm{IFFT}(\mathbf{P}_v) \otimes_N \mathbf{x} \tag{6.11}$$

where $\otimes_N$ denotes the N-point circular convolution. In other words, $\mathbf{T}_v$ is a circulant matrix corresponding to this circular convolution. Let $\mathbf{t}_v = [t_{v,0}\ t_{v,1}\cdots t_{v,N-1}]^T = \mathrm{IFFT}(\mathbf{P}_v)$. The element of $\mathbf{t}_v$ is defined as

$$\begin{aligned} t_{v,n} &= \frac{1}{N}\sum_{k=0}^{N-1} P_{v,k} e^{j\frac{2\pi kn}{N}} \\ &= \frac{1}{N}\sum_{k\in\mathbb{C}_v} e^{j\frac{2\pi kn}{N}} \end{aligned} \tag{6.12}$$

where $\mathbb{C}_v$ is the set of indices with $P_{v,k} = 1$. From (6.9) and (6.12), it is

clear that the subblock partition matrix $\mathbf{T}_v$ can be rewritten as

$$\mathbf{T}_v = [\mathbf{t}_v \ \mathbf{t}_v^{<1>} \ \mathbf{t}_v^{<2>} \cdots \mathbf{t}_v^{<N-1>}] \tag{6.13}$$

where $\mathbf{t}_v^{<\tau>}$ is a circularly down-shifted version of the column vector $\mathbf{t}_v$ by τ. From (6.13), it is easy to check that if the subblock partition vector $\mathbf{P}_v$ is given, the column vector $\mathbf{t}_v$ and the corresponding subblock partition matrix $\mathbf{T}_v$ can be determined.

Adjacent, interleaved, and random subblock partitioning schemes for the subblock partitioning of the OFDM systems can be expressed as the subblock partition matrix $\mathbf{T}_v$. However, adjacent and random partitioning schemes are not easy to implement by $\mathbf{T}_v$ because most of the elements in $\mathbf{t}_v$ are nonzero. In order words, the complexity of the circular convolution between $\mathbf{t}_v$ and $\mathbf{x}$ is much larger than that of IFFT. On the other hand, the interleaved subblock partitioning scheme is suitable for the implementation of $\mathbf{T}_v$ because there are a few nonzero elements in $\mathbf{t}_v$. The element of the subblock partition vector $\mathbf{P}_v$ for the interleaved subblock partitioning scheme is defined as

$$P_{v,k} = \begin{cases} 1, & k = Vs + v \\ 0, & \text{otherwise} \end{cases} \tag{6.14}$$

where $0 \leq s \leq N/V - 1$, $0 \leq k \leq N - 1$, and $0 \leq v \leq V - 1$. From (6.14), the element of $\mathbf{t}_v$ for the interleaved subblock partitioning scheme

is derived as

$$\begin{aligned} t_{v,n} &= \frac{1}{N}\sum_{k=0}^{N-1} P_{v,k} e^{j\frac{2\pi kn}{N}} \\ &= \frac{1}{N}\sum_{s=0}^{N/V-1} e^{j\frac{2\pi(sV+v)n}{N}} \\ &= \frac{1}{N} e^{j\frac{2\pi vn}{N}} \sum_{s=0}^{N/V-1} \left(e^{j\frac{2\pi nV}{N}}\right)^s \\ &= \begin{cases} \frac{1}{V} e^{j\frac{2\pi v}{V}l}, & n = \frac{N}{V}l \\ 0, & \text{otherwise} \end{cases} \end{aligned} \tag{6.15}$$

where $0 \le l, v \le V-1$ and $0 \le n \le N-1$. Most of the elements in $\mathbf{t}_v$ of the interleaved subblock partitioning scheme are zero except for V nonzero elements in the set $\{\frac{1}{V}e^{j\frac{2\pi}{V}\cdot 0}, \frac{1}{V}e^{j\frac{2\pi}{V}\cdot 1}, \cdots, \frac{1}{V}e^{j\frac{2\pi}{V}\cdot(V-1)}\}$. Thus, the column vector $\mathbf{t}_v$ is expressed as

$$\begin{aligned} \mathbf{t}_v = \frac{1}{V}\Bigg[&\underbrace{1\ 0\cdots 0}_{\frac{N}{V}}\ \underbrace{e^{j\frac{2\pi v}{V}}\ 0\cdots 0}_{\frac{N}{V}}\ \underbrace{e^{j\frac{2\pi v}{V}2}\ 0\cdots 0}_{\frac{N}{V}} \\ &\cdots\ \underbrace{e^{j\frac{2\pi v}{V}(V-2)}\ 0\cdots 0}_{\frac{N}{V}}\ \underbrace{e^{j\frac{2\pi v}{V}(V-1)}\ 0\cdots 0}_{\frac{N}{V}}\Bigg]^T . \end{aligned} \tag{6.16}$$

When $V = 2, 4$, the column vectors $\mathbf{t}_v$ from (6.16) are obtained as: For $V = 2$;

$$\mathbf{t}_0 = \frac{1}{2}\left[\underbrace{1\ 0\cdots 0}_{\frac{N}{2}}\ \underbrace{1\ 0\cdots 0}_{\frac{N}{2}}\right]^T$$

$$\mathbf{t}_1 = \frac{1}{2}\left[\underbrace{1\ 0\cdots 0}_{\frac{N}{2}}\ \underbrace{-1\ 0\cdots 0}_{\frac{N}{2}}\right]^T \tag{6.17}$$

and for $V = 4$;

$$\begin{aligned}
\mathbf{t}_0 &= \frac{1}{4}\left[\underbrace{1\ 0\cdots 0}_{\frac{N}{4}}\ \underbrace{1\ 0\cdots 0}_{\frac{N}{4}}\ \underbrace{1\ 0\cdots 0}_{\frac{N}{4}}\ \underbrace{1\ 0\cdots 0}_{\frac{N}{4}}\right]^T \\
\mathbf{t}_1 &= \frac{1}{4}\left[\underbrace{1\ 0\cdots 0}_{\frac{N}{4}}\ \underbrace{j\ 0\cdots 0}_{\frac{N}{4}}\ \underbrace{-1\ 0\cdots 0}_{\frac{N}{4}}\ \underbrace{-j\ 0\cdots 0}_{\frac{N}{4}}\right]^T \\
\mathbf{t}_2 &= \frac{1}{4}\left[\underbrace{1\ 0\cdots 0}_{\frac{N}{4}}\ \underbrace{-1\ 0\cdots 0}_{\frac{N}{4}}\ \underbrace{1\ 0\cdots 0}_{\frac{N}{4}}\ \underbrace{-1\ 0\cdots 0}_{\frac{N}{4}}\right]^T \\
\mathbf{t}_3 &= \frac{1}{4}\left[\underbrace{1\ 0\cdots 0}_{\frac{N}{4}}\ \underbrace{-j\ 0\cdots 0}_{\frac{N}{4}}\ \underbrace{-1\ 0\cdots 0}_{\frac{N}{4}}\ \underbrace{j\ 0\cdots 0}_{\frac{N}{4}}\right]^T .
\end{aligned} \tag{6.18}$$

In these cases, in order to generate all subblocks $\mathbf{x}_v$, $(V-1)N$ complex additions for the circular convolution of $\mathbf{t}_v$ and $\mathbf{x}$ are only required in order to generate $\mathbf{x}_v$. However, for $V > 4$, additional complex multiplications are required for a circular convolution of $\mathbf{x}$ and $\mathbf{t}_v$.

As V increases beyond 4, the computational complexity to generate $\mathbf{x}_v$ from a circular convolution of the column vector $\mathbf{t}_v$ and the OFDM signal sequence $\mathbf{x}$ considerably increases due to the complex multiplication. Thus, low complexity algorithm to implement the proposed subblock partitioning scheme in $\mathbf{x} \otimes_N \mathbf{t}_v$ will be proposed in the following section.

6.3. Low Complexity Interleaved Subblock Partitioning Scheme

In this section, two algorithms to reduce the computational complexity for the subblock partitioning scheme are proposed.

6.3.1. Subvector Rotation Scheme

Since $\mathbf{t}_v$ has only V nonzero elements, the nth element of the vth subblock $\mathbf{x}_v$ is expressed as

$$\begin{aligned} x_{v,n} &= \sum_{l=0}^{N-1} t_{v,n} x_{n-l} \\ &= \frac{1}{V} \sum_{l=0}^{V-1} e^{j\frac{2\pi v}{V}l} x_{n-\frac{N}{V}l} \end{aligned} \tag{6.19}$$

where the subscript of x_{n-l} is computed modulus N. By using the property of circular convolution, (6.19) can be written as

$$\begin{aligned} x_{v,n+\frac{N}{V}s} &= \frac{1}{V} \sum_{l=0}^{V-1} e^{j\frac{2\pi v}{V}l} x_{n+\frac{N}{V}s-\frac{N}{V}l} \\ &= e^{j\frac{2\pi v}{V}s} x_{v,n} \end{aligned} \tag{6.20}$$

where $0 \le n \le N/V - 1$ and $0 \le s \le V - 1$. Let $\mathbf{x}_v = [\mathbf{x}_v^0\ \mathbf{x}_v^1\ \cdots\ \mathbf{x}_v^{V-1}]^T$, where $\mathbf{x}_v^s = [x_{v,\frac{N}{V}s}\ x_{v,\frac{N}{V}s+1}\ \cdots\ x_{v,\frac{N}{V}(s+1)-1}]^T$, $0 \le s \le V - 1$, is the sth subvector of the vth subblock. From (6.20), the vth subblock $\mathbf{x}_v$ can be

expressed as

$$\mathbf{x}_v = \left[\mathbf{x}_v^0 \; e^{j\frac{2\pi v}{V}}\mathbf{x}_v^0 \; \cdots \; e^{j\frac{2\pi v}{V}(V-1)}\mathbf{x}_v^0\right]^T \tag{6.21}$$

where $\mathbf{x}_v^s = e^{j\frac{2\pi v}{V}s}\mathbf{x}_v^0$, $1 \le s \le V-1$ and $0 \le v \le V-1$. Note that (6.21) implies that the first N/V elements in each subblock can make other $(V-1)N/V$ elements by the phase rotation of the first N/V elements by $e^{j\frac{2\pi v}{V}s}$. As a result, the circular convolution for the first subvector of the vth subblock is only required because the remaining subvectors can be obtained directly from the phase rotation of the first subvector.

6.3.2. Reduction Algorithm of Complex Multiplication

In order to reduce the computational complexity of $\mathbf{x} \otimes_N \mathbf{t}_v$, the column vector $\mathbf{t}_v$ can be expressed as the linear combination of $V/4$ base vectors as

$$\mathbf{t}_v = \sum_{s=0}^{\frac{V}{4}-1} e^{j\frac{2\pi v}{V}s}\mathbf{t}_{v,s} \tag{6.22}$$

where

$$\mathbf{t}_{v,0} = \frac{1}{V}\left[\underbrace{1\;0\cdots0}_{\frac{N}{4}} \; \underbrace{e^{j\frac{\pi v}{2}}\;0\cdots0}_{\frac{N}{4}} \; \underbrace{e^{j\frac{\pi v}{2}2}\;0\cdots0}_{\frac{N}{4}} \; \underbrace{e^{j\frac{\pi v}{2}3}\;0\cdots0}_{\frac{N}{4}}\right]^T$$

$$\mathbf{t}_{v,1} = \frac{1}{V}\left[\underbrace{0\;0\cdots0}_{\frac{N}{V}}\underbrace{1\;0\cdots0}_{\frac{N}{4}} \; \underbrace{e^{j\frac{\pi v}{2}}\;0\cdots0}_{\frac{N}{4}} \; \underbrace{e^{j\frac{\pi v}{2}2}\;0\cdots0}_{\frac{N}{4}} \; \underbrace{e^{j\frac{\pi v}{2}3}\;0\cdots0}_{\frac{N(V-4)}{4V}}\right]^T$$

$$\mathbf{t}_{v,2} = \frac{1}{V}\left[\underbrace{0\;0\cdots0}_{\frac{2N}{V}}\underbrace{1\;0\cdots0}_{\frac{N}{4}} \; \underbrace{e^{j\frac{\pi v}{2}}\;0\cdots0}_{\frac{N}{4}} \; \underbrace{e^{j\frac{\pi v}{2}2}\;0\cdots0}_{\frac{N}{4}} \; \underbrace{e^{j\frac{\pi v}{2}3}\;0\cdots0}_{\frac{N(V-8)}{4V}}\right]^T$$

$$\vdots$$

$$\mathbf{t}_{v,\frac{V}{4}-1} = \frac{1}{V}\left[\underbrace{0\ 0\cdots 0}_{\frac{N(V-4)}{4V}}\underbrace{1\ 0\cdots 0}_{\frac{N}{4}}\ \underbrace{e^{j\frac{\pi v}{2}}\ 0\cdots 0}_{\frac{N}{4}}\ \underbrace{e^{j\frac{\pi v}{2}2}\ 0\cdots 0}_{\frac{N}{4}}\ \underbrace{e^{j\frac{\pi v}{2}3}\ 0\cdots 0}_{\frac{N}{V}}\right]^T. \tag{6.23}$$

From (6.22) and (6.23), the vth subblock $\mathbf{x}_v$ can be rewritten as

$$\begin{aligned}\mathbf{x}_v &= \mathbf{x} \otimes_N \mathbf{t}_v \\ &= \frac{1}{V}\sum_{s=0}^{\frac{V}{4}-1} \mathbf{x} \otimes_N \left(e^{j\frac{2\pi v}{V}s}\mathbf{t}_{v,s}\right) \\ &= \frac{1}{V}\sum_{s=0}^{\frac{V}{4}-1} \left(e^{j\frac{2\pi v}{V}s}\mathbf{x}\right) \otimes_N \mathbf{t}_{v,s}. \end{aligned} \tag{6.24}$$

It is easy to check that if $e^{j\frac{2\pi v}{V}s}\mathbf{x}$, $1 \le s \le \frac{V}{4}-1$, is calculated and saved, additional complex multiplications are not required for this circular convolution because the elements of base vectors in $\mathbf{t}_v$ take the values in $\{\pm 1, \pm j\}$. In other words, generating all V subblocks only requires $\left(\frac{V}{4}-1\right)N$ complex multiplications.

6.4. Analysis of Computational Complexity

In this section, the computational complexity to generate the vth subblock $\mathbf{x}_v$ from subblock partition matrices is analyzed. In the proposed subblock partitioning scheme, one N-point IFFT operation for an input symbol sequence is needed to generate V subblocks. Table I compares the

Table 6.1: Computational complexity of the random, the interleaved, and the proposed subblock partitioning schemes with V subblocks.

	Total number of complex multiplications	Total number of complex additions
Random subblock partitioning scheme	$\frac{VN}{2}\log_2 N$	$VN\log_2 N$
Interleaved subblock partitioning	$\frac{N}{2}\log_2 \frac{N}{V} + (V-1)N$	$N\log_2 \frac{N}{V}$
Proposed subblock partitioning ($V = 2, 4$)	$\frac{N}{2}\log_2 N$	$N\log_2 N + (V-1)N$
Proposed subblock partitioning ($V > 4$)	$\frac{N}{2}\log_2 N + \left(\frac{V}{4} - 1\right) N + (V-4)\left(\frac{V}{4} - 1\right)\frac{N}{V}$	$N\log_2 N + (V-1)N$

computational complexity of the random, the interleaved, and the proposed partitioning schemes for the OFDM system. It is assumed that the number of complex multiplications and additions of the N-point IFFT are $(N/2)\log_2 N$ and $N\log_2 N$, respectively. In addition, we assume that the multiplication between each signal element and elements in $\{\pm 1, \pm j\}$ is ignored.

The random subblock partitioning scheme requires V IFFT operations to generate V subblocks. Thus, the number of required complex multiplications and complex additions for the random subblock partitioning scheme are $(VN/2)\log_2 N$ and $VN\log_2 N$, respectively. On the other hand, the interleaved subblock partitioning scheme can utilize the reduced

N/V-point IFFT operation as follows:

$$\begin{aligned} x_{v,n} &= \frac{1}{\sqrt{N}} \sum_{k=0}^{N-1} X_{v,k} e^{j\frac{2\pi kn}{N}} \\ &= \frac{1}{\sqrt{N}} \sum_{s=0}^{\frac{N}{V}-1} X_{v,Vs+v} e^{j\frac{2\pi(Vs+v)n}{N}} \\ &= \frac{1}{\sqrt{N}} e^{j\frac{2\pi vn}{N}} \sum_{s=0}^{\frac{N}{V}-1} X_{v,Vs+v} e^{j\frac{2\pi sn}{N/V}}. \end{aligned} \tag{6.25}$$

Equation (6.25) tells us that $(N/2V)\log_2 N/V + N$ complex multiplications and $(N/V)\log_2 N/V$ complex additions are required for each subblock in the interleaved subblock partitioning scheme. Since the subblock $\mathbf{x}_0$ for $v = 0$ is obtained without N complex multiplications, the total number of the required complex multiplications and complex additions in the interleaved subblock partitioning scheme are $((N/2)\log_2 N/V + (V-1)N$ and $N\log_2 N/V$.

For the proposed subblock partitioning scheme, by applying $\mathbf{x} \otimes_N \mathbf{t}_v$, the number of N and $3N$ complex additions to obtain V subblocks without additional complex multiplications is required for $V = 2$ and 4, respectively. When $V > 4$, the total number of the required complex additions is still $N\log_2 N + (V-1)N$, but complex multiplications are needed as follows. First, complex multiplications are involved to calculate $e^{j\frac{2\pi v}{V}s}\mathbf{x}$, $1 \le s \le \frac{V}{4} - 1$, in (6.24). To generate the next $N(V-1)/4V$ elements using the computation of the first N/V elements of each subblock in (6.21), $N(V-1)/4V$ complex multiplications are required. By using $N/4$ elements of each subblock in (6.21), the remaining $3N/4$ el-

ements are obtained by the multiplication of elements in $\{\pm 1, \pm j\}$. For $v = Vl/4, l = 0, 1, 2, 3$, these complex multiplications are not required because $e^{j\frac{2\pi v}{V}s} \in \{\pm 1, \pm j\}$, $0 \leq s \leq V-1$ in (6.21). Therefore, to generate V subblocks for $V > 4$, the total number of the required complex multiplications is $(N/2)\log_2 N + (V/4-1)N + (V-4)(V/4-1)N/V$.

Fig. 6.2 compares the computational complexity of the random, the interleaved, and the proposed subblock partitioning schemes for $N = 1024$. In Fig. 6.2, it is checked that the number of complex multiplications required in the proposed scheme is less than that of the random and interleaved subblock partitioning schemes. On the other hand, the number of complex additions for the proposed subblock partitioning scheme slightly increases compared to that of the interleaved subblock partitioning scheme.

To fairly compare the proposed scheme with other subblock partitioning schemes, we consider the total number of flops to provide complex multiplications and complex additions. It is known that each complex multiplication and complex addition involve 6 flops and 2 flops, respectively. Fig. 6.3 compares the total number of flops for the random, the interleaved, and the proposed subblock partitioning schemes with $N = 1024$. From Fig. 6.3, it is shown that the computational complexity to generate V subblocks can be minimized in the proposed subblock partitioning scheme.

6.5. Conclusion

In this chapter, a new subblock partitioning scheme using the subblock partition matrix is proposed. Using the convolution property of the IFFT, the subblock partition vector for the interleaved subblock partitioning scheme consists of $N - V$ zero elements and V nonzero elements. The complexity of the proposed subblock partitioning scheme is lower than that of the random and the interleaved subblock partitioning schemes. When $V = 2, 4$, additional $(V-1)N$ complex additions to generate a signal subsequence are required. For $V > 4$, since complex multiplications to calculate the circular convolution are needed, the algorithm to reduce the computational complexity for the proposed subblock partitioning scheme is proposed.

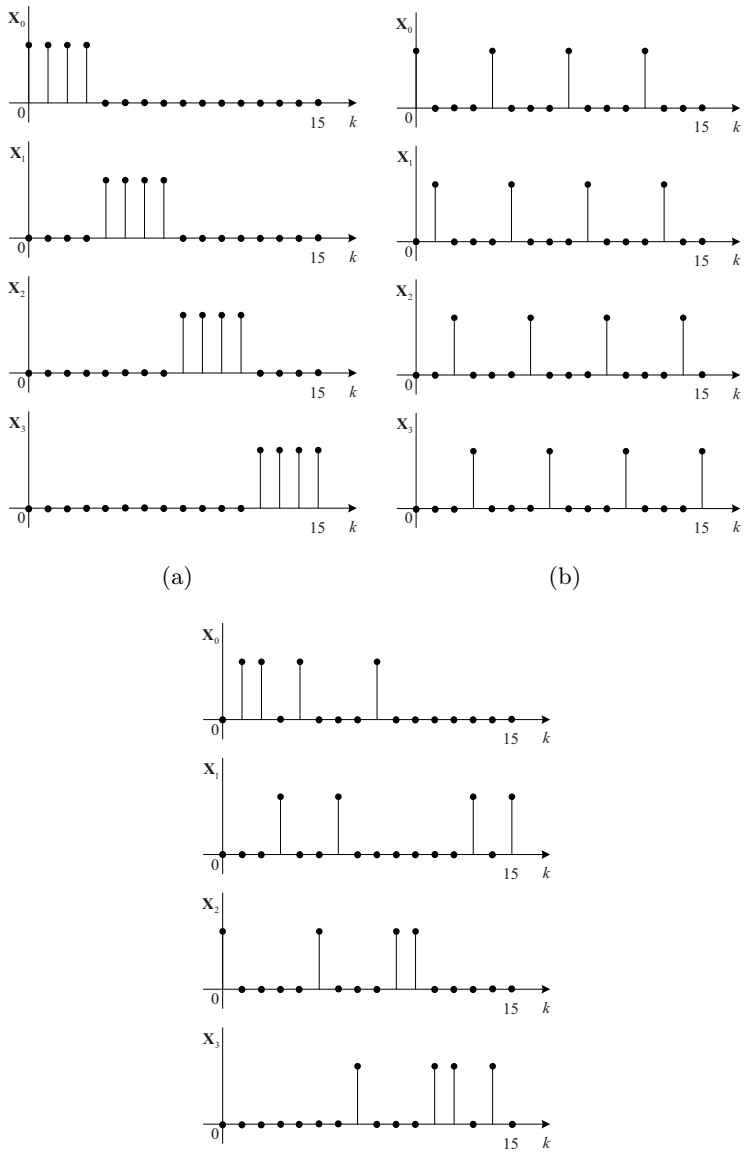

Figure 6.1: Example of three subblock partitioning schemes with $N = 16$ and $V = 4$: (a) Adjacent subblock partitioning scheme, (b) interleaved subblock partitioning scheme, (c) random subblock partitioning scheme.

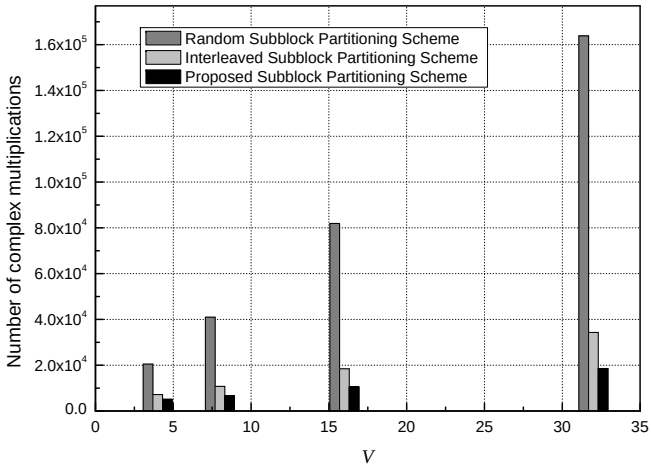

(a)

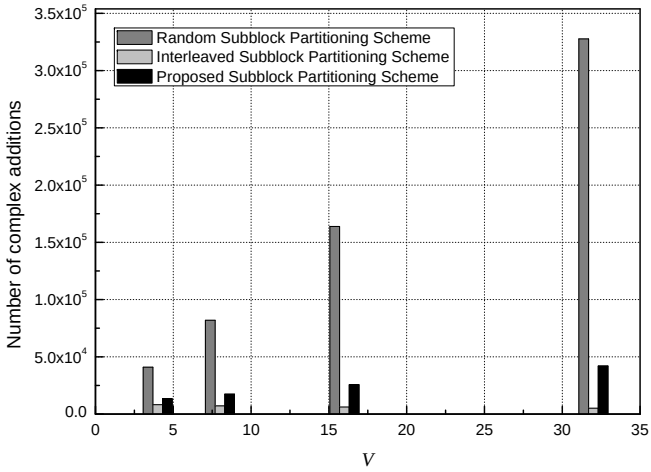

(b)

Figure 6.2: Comparison of the computational complexity of the random, the interleaved, and the proposed subblock partitioning schemes for $N = 1024$ with $U = 4, 8, 16$, and 32: (a) The number of complex multiplications, (b) the number of complex additions.

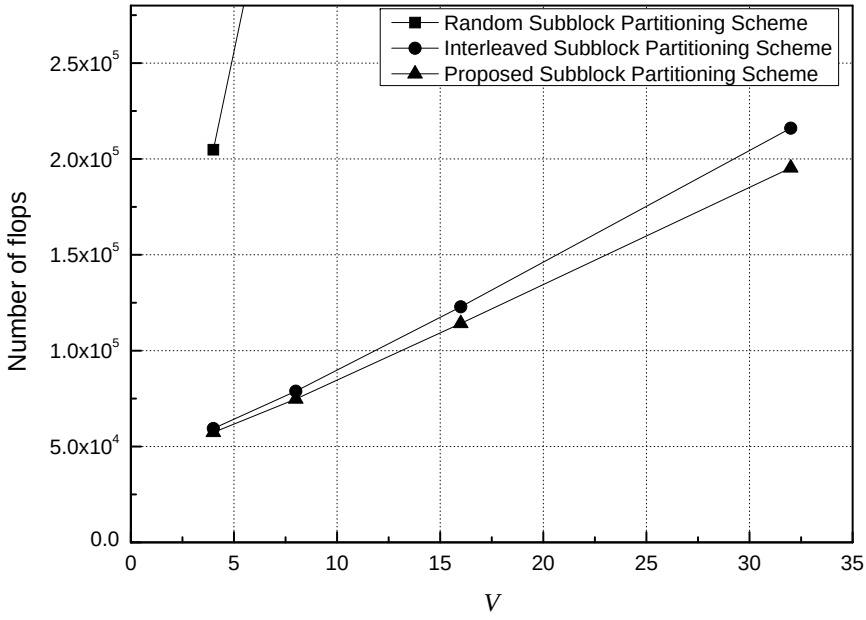

Figure 6.3: Comparison of the number of flops in the interleaved and the proposed subblock partitioning schemes for $N = 1024$ with $U = 4, 8, 16,$ and 32.

Chapter 7. Conclusions

In this dissertation, we reviewed OFDM system and their PAPR characteristics. To solve PAPR problem of OFDM system, several PAPR reduction schemes have been proposed. These PAPR reduction schemes such as coding, clipping and filtering, SLM, PTS, and TR are introduced and have their own characteristics and trade-off. Then, we proposed the blind PAPR reduction schemes with low complexity to overcome some disadvantages.

In Chapter 4, a new BSLM scheme with low decoding complexity was proposed for PAPR reduction of OFDM signals. In the proposed BSLM scheme, the side information is embedded into each phase sequence by giving the phase offset to the elements of phase sequences, which are determined by the biorthogonal vectors for the partitioned subblocks. Also, the proposed BSLM scheme reduces the decoding complexity by $(U-2)/U$ compared to the conventional BSLM scheme. The numerical results show that for QPSK and 16-QAM, the BER and the PAPR reduction performances of the proposed BSLM scheme are almost the same as those of the conventional BSLM scheme. Due to the reduced decoding complexity, the proposed BSLM scheme is practically better than the conventional BSLM scheme, especially for the high data rate OFDM systems.

In Chapter 5, we proposed two BPTS schemes without side information for PAPR reduction of OFDM signals. The proposed BPTS schemes embed the side information identifying a rotating vector into itself by using the phase offset on the elements of each rotating vector. To find side information of the rotating vector and recover the data sequence, the ML decoders for the proposed BPTS schemes are derived. By using PEP analysis, the selected phase offsets in each BPTS scheme is described. The simulation results show that for QPSK and 16-QAM, the BER performance of the proposed BPTS schemes are not degraded.

In Chapter 6, we proposed a new subblock partitioning scheme using the subblock partition matrix. Based on the convolution property of the IFFT, the subblock partition vector for the interleaved subblock partition consists of $N - V$ zero elements and V nonzero elements. The complexity of the proposed subblock partitioning scheme is lower than that of the random and interleaved subblock partitioning scheme. When $V = 2, 4$, additional $(V - 1)N$ complex additions to generate a signal subsequence are required. For $V > 4$, since compelx multiplications to calculate the circular convolution are needed, the algorithm to reduce the computational complexity for the proposed subblock partitioning scheme is proposed.

Bibliography

[1] R. W. Chang and R. A. Gibby, "A theoretical study of performance of an orthogonal multiplexing data transmission scheme," *IEEE Trans. Commun.*, vol. COM-16, no. 4, Aug. 1968.

[2] S. B. Weinstein and P. M. Erbert, "Data transmission by frequency-division multiplexing using the discrete Fourier transform," *IEEE Trans. Commun.*, vol. COM-19, pp. 628–634, Oct. 1971.

[3] A. Peled and A.Ruiz, "Frequency domain data transmission using reduced computational complexity algorithms," in *Proc. IEEE ICASSP,* vol. 5, Apr. 1980, pp. 964–967.

[4] R. van Nee and R. Prasad, *OFDM for Wireless Multimedia Communications*. Boston, MA: Arthech House, 2000.

[5] D. Wulich and L. Goldfeld, "Reduction of peak factor in orthogonal multicarrier modulation by amplitude limiting and coding," *IEEE Trans. Commun.*, vol. 47, no. 1, pp. 18–21, Jan. 1999.

[6] J. Tellado and J. M. Cioffi, *Multicarrier Modulation with Low PAR: Appication to DSL and Wireless*. Boston, MA: Kluwer Academic Publisher, 2000.

[7] R. W. Bäuml, R. F. H. Fischer, and J. B. Huber, "Reducing the peak-to-average power ratio of multicarrier modulation by selected mapping," *Electron. Lett.*, vol. 32, no. 22, pp. 2056–2057, Oct. 1996.

[8] S. H. Müller, R. W. Bäuml, R. F. H. Fischer, and J. B. Huber, "OFDM with reduced peak-to-average power ratio by multiple signal representation," *Ann. Telecommun.*, vol. 52, no. 1–2, pp. 58–67, Feb. 1997.

[9] R. J. Baxley and G. T. Zhou, "Comparing selected mapping and partial transmit sequence for PAPR reduction," *IEEE Trans. Broadcast.*, vol. 53, no. 4, pp. 797–803, Dec. 2007.

[10] H.-B. Jeon, K.-H. Kim, J.-S. No, and D.-J. Shin, "Bit-based SLM schemes for PAPR reduction in QAM modulated OFDM signals," *IEEE Trans. Broadcast.*, vol. 55, no. 3, pp. 679–685, Sep. 2009.

[11] H.-B. Jeon, J.-S. No, and D.-J. Shin, "A low-complexity SLM scheme using additive mapping sequences for PAPR reduction of OFDM signals," *IEEE Trans. Broadcast.*, vol. 57, no. 4, pp. 866–875, Dec. 2011.

[12] S.-J. Ku, C.-L. Wang, and C.-H. Chen, "A reduced-complexity PTS-based PAPR reduction scheme for OFDM systems," *IEEE Trans. Wireless Commun.*, vol. 9, no. 8, pp. 2455–2460, Aug. 2010.

[13] R. J. Baxley and G. T. Zhou, "Map metric for blind phase sequence detection in seleted mapping," *IEEE Trans. Broadcast.*, vol. 51, no. 4, pp. 565–570, Dec. 2005.

[14] S. Y. Le Goff, S. S. Al-Samahi, B. K. Khoo, C. C. Tsimenidis, and B. S. Sharif, "Selected mapping without side information for PAPR reduction in OFDM," *IEEE Trans. Wireless Commun.*, vol. 8, no. 1, pp. 3320–3325, Jul. 2009.

[15] A. D. S. Jayalath and C. Tellambura, "SLM and PTS peak-power reduction of OFDM signals without side information," *IEEE Trans. Wireless Commun.*, vol. 4, no. 5, pp. 2006–2013, Sep. 2005.

[16] H. Kim, E. Hong, C. Ahn, and D. Har "A pilot symbol pattern enabling data recovery without side information in PTS-based OFDM systems," *IEEE Broadcast.*, vol. 57, no. 2, pp. 307–312, Jun. 2011.

[17] A. A. M. Saleh, "Frequency-independent and frequency-dependent nonlinear models of TWT amplifiers," *IEEE Trans. Commun.,* vol. 29, no. 11, pp. 1715–1720, Nov. 1981.

[18] C. Rapp, "Effects of HPA nonlinearity on a 4-DPSK/OFDM signal for a digital sound broadcasting system," in *Proc. Int. Conf. Digital Process. Signals Commun.,* Sep. 1991, vol. 1, pp. 193–197, Leicestershire, UK.

[19] M. Sharif, M. Gharavi-Alkhansari, and B. H. Khalaj, "On the peak to average power of OFDM signals based on oversampling," *IEEE Trans. Commun.*, vol. 51, no. 1, pp. 72–78, Jan. 2003.

[20] R. van Nee and A. de Wild, "Reducing the peak-to-average power ratio of OFDM," in *Proc. VTC*, May 1998, pp. 2072–2076.

[21] H. Ochiai and H. Imai, "On the distribution of the peak-to-average power ratio in OFDM signals," *IEEE Trans. Commun.*, vol. 49, no. 2, Feb. 2001.

[22] J. Amstrong, "Peak to average power reduction for OFDM by repeated clipping and fequency domain filtering," *IEE Electron. Lett.*, vol. 38, no. 5, pp. 246–247, Feb. 2002.

[23] X. Li and L. J. Cimini Jr., "Effects of clipping and filtering on the performance of OFDM," *IEEE Commun. Lett.,* vol.2, no. 5. pp. 131–133, May 1998.

[24] B. S. Krongold and D. L. Jones, "PAR reduction in OFDM via active constellation extension," *IEEE Trans. Broadcast.*, vol. 49, no. 3, pp. 258–268, Sep. 2002.

[25] A. E. Jones, T. A. Wilkinson, and S. K. Barton, "Block coding scheme for reduction of peak to mean envelope power ratio of multicarrier transmission schemes," *IET Electron. Lett.*, vol. 30, no. 25, pp. 2098–2099, Dec. 1994.

[26] R. van Nee, "OFDM codes for peak-to-average power reduction and error correction," in *Proc. GLOBECOM*, Nov. 1996, pp. 740–744.

[27] J. A. Davis and J. Jedwab, "Peak-to-mean power control in OFDM, Golay complementary sequences, and Reed-Muller codes," *IEEE Trans. Inf. Theory*, vol. 45, no. 7, pp. 2397–2417, Nov. 1999.

[28] K. G. Paterson and V. Tarokh, "On the existence and construction of good codes with low peak-to-average power ratios," *IEEE Trans. Inf. Theory*, vol. 46, no. 6, pp. 1974–1987, Sep. 2000.

[29] D.-W. Lim, C.-W. Lim, J.-S. No, and H. Chung, "A new SLM OFDM with low complexity for PAPR reduction," *IEEE Signal Process. Lett.*, vol. 12, no. 2, pp. 93–96, Feb. 2005.

[30] C.-L. Wang and Y. Ouyang, "Low-complexity selected mapping schemes for peak-to-average power ratio reduction in OFDM systems," *IEEE Trans. Signal Process.*, vol. 53, no. 12, pp. 4652–4660, Dec. 2005.

[31] C.-L. Wang and S.-J. Ku, "Novel conversion matrices for simplifying the IFFT computation of an SLM-based PAPR reduction scheme for OFDM systems," *IEEE Trans. Commun.*, vol. 57, no. 7, pp. 1903–1907, Jul. 2009.

[32] C.-P. Li, S.-H. Wang, and C.-L. Wang, "Novel low-complexity SLM schemes for PAPR reduction in OFDM systems," *IEEE Trans. Signal Process.*, vol. 58, no. 5, pp. 2916–2921, May 2010.

[33] D.-W. Lim, S.-J. Heo, J.-S. No, and H. Chung, "A new PTS OFDM scheme with low complexity for PAPR reduction," *IEEE Trans. Broadcast.*, vol. 52, no. 1, pp. 77–82, Mar. 2006.

[34] G. T. Zhou and L. Peng, "Optimality condition for selected mapping in OFDM," *IEEE Trans. Signal Process.*, vol. 54, no. 8, pp. 3159–3165, Aug. 2006.

[35] D.-W. Lim, S.-J. Heo, J.-S. No, and H. Chung, "On the phase sequence set of SLM OFDM scheme for a crest factor reduction," *IEEE Trans. Signal Process.*, vol. 54, no. 5, pp. 1931–1935, May 2006.

[36] F. J. Macwilliams and N. J. A. Sloane, *The Theory of Error-Correcting Codes*. Amsterdam, Netherlands:North-Holland, 1981.

[37] V. Tarokh, N. Seshadri, and A. R. Calderbank, "Space-time codes for high data rate wireless communications: Performance criterion and code construction," *IEEE Trans. Inf. Theory*, vol. 44, no. 2, pp. 744–765, Mar. 1998.

[38] D. L. Goeckel and G. Ananthaswamy, "On the design of multidimensional signal sets for OFDM systems," *IEEE Trans. Commun.*, vol. 50, no. 3, MAR. 2002.

[39] J. G. Proakis, *Digital Communicatioins.* New York: McGraw-Hill, 2008.

[40] A. V. Oppenheim and R. W. Schafer, *Discrete-Time Signal Processing*. 3rd ed., Prentice Hall, 2009.

[41] S. G. Kang, J. G. Kim, and E. K. Joo, "A novel subblock partition scheme for partial transmit sequence OFDM," *IEEE Trans. Broadcast.*, vol. 45, no. 3, pp. 333–338, Sep. 1999.

초 록

본 논문은 직교주파수분할다중화 시스템의 최대전력대평균전력비를 감소시키는 블라인드 SLM 및 PTS 기법들을 제안한다. 먼저 서두에서는 직교주파수분할다중화 시스템의 기본원리와 성능 및 구현방법 등을 살펴본다. 다음으로 비선형고출력전력증폭기의 특성을 직교주파수분할다중화 시스템의 큰 단점인 최대전력대평균전력비을 고려하여 분석 설명한다. 직교주파수분할다중화 시스템의 최대전력대평균전력비를 감소시키는 기법에 관한 연구가 지금까지 활발히 진행되어 왔으며 대표적인 방법으로는 클리핑기법, 피크 제거 기법, 부호화기법, 선택 사상 기법, 부분 전송 수열 기법, 톤 예약 기법, 톤 삽입 기법 등이 있다.

본 논문에서 제안한 최대전력대평균전력의비 감소 방법들은 다음과 같다. 먼저, 적은 복잡도를 가지는 새로운 블라인드 SLM 기법을 제안한다. 이 방법은 적은 복호 복잡도를 가지고 있고 약간의 비트오류율 성능만을 열화 시킨다. 부가 정보를 OFDM 심볼에 실어 전송하기 위해 구간 분할과 위상 회전을 이용한다. 수신단에서 부가 정보를 찾기 위해서는 최대 우도 복호기를 이용한다. 이 블라인드 SLM 방법은 BER 성능 열화가 거의 없고 기존의 SLM과 동일한 PAPR 감소 성능을 가지고 있다.

다음으로는 제안된 블라인드 SLM 기법을 확장시킨 새로운 블라인드 PTS 기법을 제안한다. 블라인드 SLM에 적용했던 알고리듬을 PTS의 회전 인자에 적용하여 대안의 신호의 회전 인자마다 정해진 위상 오프셋을 주고 수신단에서는 이러한 위상 오프셋으로부터 부가 정보를 찾기 위해 최대 우도 복호기를 이용한다.

상기의 방법 중 PTS의 송신단 복잡도를 감소시키기 위해 이산 신호

성질을 이용한 부분할 행렬을 제안한다. 이 방법을 이용하면 단 한번의 IFFT 및 추가적인 연산만으로 송신단에서 부분할 신호 시퀀스들을 얻어낼 수 있어 적은 연산량으로 PTS 구현이 가능하고 SFBC와 OFDMA 시스템으로도 확장이 가능한 장점을 가진다.

주요어: 부가 정보, 부분전송수열, 선택사상기법, 직교주파수분할다중화, 최대전력대평균전력비.
학번: 2008-30888